Synchronization in adaptive higher-order networks

Anwar, Md Sayeed; Selvaraj, Nirmala Jenifer; Muruganandam, Paulsamy; Ghosh, Dibakar; Carletti, Timoteo

Published in:
Physical Review. E : Statistical, Nonlinear, and Soft Matter Physics

DOI:
10.1103/physreve.110.064305

Publication date:
2024

Document Version
Peer reviewed version

Synchronization in adaptive higher-order networks

Md Sayeed Anwar,[1,2,*] S. Nirmala Jenifer,[3] Paulsamy Muruganandam,[3] Dibakar Ghosh,[1] and Timoteo Carletti[2,†]

[1] *Physics and Applied Mathematics Unit, Indian Statistical Institute, 203 B. T. Road, Kolkata 700108, India*
[2] *Department of Mathematics and Namur Institute for Complex Systems, naXys, University of Namur, 2 rue Grafé, Namur B5000, Belgium*
[3] *Department of Physics, Bharathidasan University, Tiruchirappalli 620024, Tamil Nadu, India*

Many natural and human-made complex systems feature group interactions that adapt over time in response to their dynamic states. However, most of the existing adaptive network models fall short of capturing these group dynamics, as they focus solely on pairwise interactions. In this study, we employ adaptive higher-order networks to describe these systems by proposing a general framework by incorporating both adaptivity and group interactions. We demonstrate that global synchronization can exist in those complex structures and we provide the necessary conditions for the emergence of a stable synchronous state. We first study the setting in which both pairwise and higher order interactions are allowed, but only the former adapt in time, then we extend this framework by considering also higher order adaptive interactions. In both analyzed settings we show that the necessary condition is strongly related to the master stability equation, allowing to separate the dynamical and structural properties. We illustrate our theoretical findings through the relevant examples involving adaptive higher-order networks of coupled generalized Kuramoto oscillators with phase lag, coupled with an all-to-all and a nonlocal ring–like structure. We also show that the interplay of group interactions and adaptive connectivity results in the formation of stability regions that can induce transitions between synchronization and desynchronization. Our findings also reveal that the introduction of higher-order adaptation significantly alters the synchronization stability when compared with the case with constant higher-order interactions.

I. INTRODUCTION

In the realm of complex systems, synchronization is a captivating and widespread phenomenon where coupled systems spontaneously self-organize by displaying a coordinated behavior [1, 2]. This phenomenon, emerging in both natural and artificial systems, has long intrigued scientists seeking to understand its underlying principles [3].

Network science has emerged as a powerful framework for studying synchronization, where interconnected nonlinear oscillators are represented as nodes, and their interactions as pairwise links [4]. However, traditional network models have limitations when applied to many natural and human-made systems, such as brain networks [5] and social networks [6], where connections between individual units are dynamic and evolve over time. To address this issue, the concept of networks has been generalized as to include temporally evolving connectivity topology [7]. A particularly intriguing class of these generalized network structures is given by the adaptive networks, where the temporal evolution of the network structure is intricately linked to the dynamical state of its nodes, leading to the coevolution of both the network topology and its individual components [8–11]. For example, synaptic connections between neurons adjust based on the relative timing of neuronal spikes [12–15]. Likewise, in certain chemical systems, reaction rates dynamically adapt according to the system variables [16]. Activity-dependent plasticity is also prevalent in epidemics and various biological or social systems [17, 18]. Researchers have investigated synchronization within adaptive networks [19–26], as well as in conventional time-varying networks [27–31], where the temporal evolution of connections is predefined and independent of node dynamics.

Another limitation of traditional network models is their focus on pairwise interactions, which fails to capture the complexity of many real-world systems. To overcome this limitation, researchers have highlighted the importance of higher-order structures that go beyond pairwise links by allowing for simultaneous interactions among multiple agents [32–35]. Higher-order structures, such as simplicial complexes [36] and hypergraphs [37], offer a more nuanced understanding of complex systems and have revealed new features in various dynamical processes, including epidemics [38], random walks [39, 40], consensus [41], pattern formation [42, 43], synchronization [44–54], swarmalation [55] and more [56, 57].

Despite these advances, the current frameworks still fall short in describing systems with both adaptivity and higher-order interactions. For instance, in neuronal networks, a group of neurons interact simultaneously [58, 59] and also, the synaptic connectivity between them depends on the neuronal spike timing [13–15]. In this work, we thus aim to close this gap by exploring the interplay between higher-order and adaptive interactions by proposing a general framework for studying synchronization involving nonlinear oscillators coupled via adaptive higher-order network structures. To the best of our knowledge, only a few recent studies have explored the adaptive nature of higher-order interactions and their effects on the synchronization process [60–63]. For in-

* sayeedanwar447@gmail.com
† timoteo.carletti@unamur.be

stance, it has been shown that group interactions in adaptive networks can influence synchronization transitions within the Kuramoto model [61, 62]. Let us observe that these studies have restricted their focus on the Kuramoto model and have been limited to examining only the routes to transitions between synchronization and desynchronization, such as continuous or abrupt transitions.

In this work, we overcome the limitations of the above-cited results and introduce a broad framework for studying dynamical systems within adaptive higher-order networks. Specifically, we consider a finite ensemble of generic (but identical) dynamical systems anchored to the nodes of an adaptive higher-order network, where the interactions are governed by general coupling functions. For simplicity, we focus on simultaneous interactions up to three bodies, but the proposed framework can be easily extended as to accommodate for interactions of any order. Within such context, we examine the synchronization, specifically global synchronization in adaptive higher-order networks. This approach extends the study by Berner et al. [19] on synchronization in adaptive networks to the domain of higher-order networks. Given the existence of a synchronous solution, we derive the necessary conditions for its stability in two scenarios: first, when only the pairwise connections adapt according to node dynamics while higher-order connections remain fixed, and second, when both pairwise and higher-order connections adapt based on node dynamics. We considered a couple of relevant higher-order structures, all-to-all and ring-like, and we shown that the analytical stability conditions we derived, resemble the Master Stability Equation (MSE) approach [64, 65]. This is a method originally developed for static pairwise networks, and since then extended to various complex networks, including time-varying networks [29, 30, 66] and static higher-order networks [49, 51]. To validate the analytic derivations we obtained, we use the generalized Kuramoto model with phase lag defined on adaptive higher-order networks. We show how the combined effect of adaptivity and higher-order interactions change the stability of the synchronous state. We also demonstrate that the interplay between adaptation and group interactions can lead to the formation of stability regions, which induce transitions between synchronization and desynchronization.

II. ADAPTIVE PAIRWISE AND STATIC HIGHER-ORDER INTERACTIONS

Let us first consider the case where both pairwise and higher-order interactions are present, but only the former can evolve in time as a function of the system state variables; the three-body terms are thus supposed to be given by a stationary tensor. More precisely, we are considering the system,

$$\begin{aligned}\dot{\mathbf{x}}_i =& f(\mathbf{x}_i) - \sigma_1 \sum_{j=1}^{N} a_{ij}^{(1)} k_{ij}^{(1)}(t) g^{(1)}(\mathbf{x}_i, \mathbf{x}_j) \\ & - \sigma_2 \sum_{j=1}^{N}\sum_{p=1}^{N} a_{ijp}^{(2)} k_{ijp}^{(2)} g^{(2)}(\mathbf{x}_i, \mathbf{x}_j, \mathbf{x}_p)\,, \end{aligned} \tag{1}$$

where the smooth function f (assumed to be same for all nodes) describes the dynamics of d-dimensional isolated nodes, $a_{ij}^{(1)}$ (resp. $a_{ijp}^{(2)}$), is the adjacency matrix (resp. adjacency 2-tensor) encoding for the "topological" pairwise (resp. three-body) interactions, namely for the possible interactions among the constituting basic units despite their actual realization due to the adaptation of the structures. The time-varying matrix $k_{ij}^{(1)}(t)$ describes the adaptation of the weight links due to the time evolution of the state variables. The 2-tensor $k_{ijp}^{(2)}$ encodes for the weights of the three-body interaction; let us observe that for the time being, we assume it to be constant and thus we could have merged it with $a_{ijp}^{(2)}$, we, however, preferred to keep them separate from each other to use a similar notation in the following section, where also the higher-order interactions can adapt to the system state evolution. Finally, the function $g^{(1)}$ (resp. $g^{(2)}$) encodes the coupling involving two-body (resp. three-body) and σ_j, $j = 1, 2$, denote the corresponding coupling strengths.

As already stated, weights of pairwise interactions adapt because of the evolution of the system state [19, 67, 68], more precisely, we assume for all $i, j \in \{1, 2, \ldots, N\}$,

$$\dot{k}_{ij}^{(1)} = -\epsilon[k_{ij}^{(1)} + a_{ij}^{(1)} h(\mathbf{x}_i - \mathbf{x}_j)]\,, \tag{2}$$

for some scalar coupling function h and $0 < \epsilon \ll 1$ is a parameter that separates the time scales of the slow dynamics of the coupling strengths from the fast dynamics of the oscillatory system. On the other hand, we assume the strengths of the higher-order interactions to be fixed over time,

$$k_{ijp}^{(2)} = 1 \quad \forall i, j, p \in \{1, 2, \ldots, N\}\,. \tag{3}$$

Without any further assumption on the coupling functions, we require the following to hold true for the synchronization to occur

1. $\sum_{j=1}^{N} a_{ij}^{(1)} = r^{(1)}$, i.e., each node must participate in the same number of pairwise interactions.

2. $\sum_{j=1}^{N}\sum_{p=1}^{N} a_{ijp}^{(2)} = 2r^{(2)}$, i.e., each node must participate in the same number of triadic interactions.

Stated differently, we are assuming that the pairwise structure, $a_{ij}^{(1)}$, and the higher-order one, $a_{ijp}^{(2)}$, are regular. This assumption of constant degree is essential to enable synchronization for generic coupling functions.

Let us observe that we can overcome the above limitation of constant degree by considering the coupling functions $g^{(1)}$ and $g^{(2)}$ to be synchronization noninvasive, i.e., $g^{(1)}(\mathbf{s},\mathbf{s}) = 0$ and $g^{(2)}(\mathbf{s},\mathbf{s},\mathbf{s}) = 0$. By imposing the noninvasive condition on the coupling functions, we can accommodate any network topology to achieve global synchronization. A detailed study of this case will be provided in Appendix A.

A. Emergence of synchronization

Based on the above, we can look for a global synchronous solution $\mathbf{s}(t)$ of the system described by Eqs. (1) - (2), namely a solution independent from the nodes indexes, it then follows that the latter should satisfy

$$\dot{\mathbf{s}} = f(\mathbf{s}) + \sigma_1 r^{(1)} h(0) g^{(1)}(\mathbf{s},\mathbf{s}) - 2\sigma_2 r^{(2)} g^{(2)}(\mathbf{s},\mathbf{s},\mathbf{s}), \quad (4)$$

$$k_{ij}^{(s)} = -a_{ij}^{(1)} h(0)\,. \quad (5)$$

To analyze the stability of this synchronous state, we perform linear stability analysis; namely, we consider perturbations of the form $\xi_i = \mathbf{x}_i - \mathbf{s}$ and $\chi_{ij} = k_{ij}^{(1)} - k_{ij}^{(s)}$, whose time evolution is obtained by solving

$$\begin{aligned}
\dot{\xi}_i =& Df(\mathbf{s})\xi_i - \sigma_1 \sum_{j=1}^{N} a_{ij}^{(1)} g^{(1)}(\mathbf{s},\mathbf{s})\chi_{ij} + \sigma_1 r^{(1)} h(0)[D_1 g^{(1)}(\mathbf{s},\mathbf{s}) + D_2 g^{(1)}(\mathbf{s},\mathbf{s})]\xi_i + \\
&- \sigma_1 h(0) \sum_{j=1}^{N} L_{ij}^{(1)} D_2 g^{(1)}(\mathbf{s},\mathbf{s})\xi_j - 2\sigma_2 r^{(2)}[D_1 g^{(2)}(\mathbf{s},\mathbf{s},\mathbf{s}) + D_2 g^{(2)}(\mathbf{s},\mathbf{s},\mathbf{s}) + D_3 g^{(2)}(\mathbf{s},\mathbf{s},\mathbf{s})]\xi_i + \\
&+ \sigma_2 \sum_{j=1}^{N} L_{ij}^{(2)}[D_2 g^{(2)}(\mathbf{s},\mathbf{s},\mathbf{s}) + D_3 g^{(2)}(\mathbf{s},\mathbf{s},\mathbf{s})]\xi_j, \quad (6)
\end{aligned}$$

$$\dot{\chi}_{ij} = -\epsilon\left(\chi_{ij} + a_{ij}^{(1)}[Dh(0)(\xi_i - \xi_j)]\right), \quad (7)$$

where $\mathbf{L}^{(1)}$ and $\mathbf{L}^{(2)}$ are the Laplace matrices for pairwise and three-body interactions, namely

$$L_{ij}^{(1)} = \begin{cases} -a_{ij}^{(1)}, & i \neq j \\ \sum_{j=1}^{N} a_{ij}^{(1)} = r^{(1)}, & i = j \end{cases} \quad (8)$$

and,

$$L_{ij}^{(2)} = \begin{cases} -\sum_{k=1}^{N} a_{ijk}^{(2)}, & i \neq j \\ \sum_{j=1}^{N}\sum_{k=1}^{N} a_{ijk}^{(2)} = 2r^{(2)}, & i = j. \end{cases} \quad (9)$$

$D_i g^{(j)}$ denotes the Jacobian of the function $g^{(j)}$, $j = 1, 2$, with respect to the i-th variables, $i = 1, 2, 3$.

To write the previous equations into a more compact form, we assume to cast the $N \times N$ matrix χ_{ij} into a N^2-dimensional vector by stacking the rows on rows successively, i.e., $\boldsymbol{\chi} = (\chi_{11}, \ldots, \chi_{1N}, \chi_{21}, \ldots, \chi_{2N}, \ldots, \chi_{N1}, \ldots, \chi_{NN})^\top$. We can thus rewrite Eqs. (6) and (7) as follows,

$$\begin{bmatrix} \dot{\boldsymbol{\xi}} \\ \dot{\boldsymbol{\chi}} \end{bmatrix} = \begin{bmatrix} \mathbf{S} & -\sigma_1 \mathbf{B}^{(1)} \otimes g^{(1)}(\mathbf{s},\mathbf{s}) \\ -\epsilon \mathbf{C}^{(1)} \otimes Dh(0) & -\epsilon \mathbf{I}_{N^2} \end{bmatrix} \begin{bmatrix} \boldsymbol{\xi} \\ \boldsymbol{\chi} \end{bmatrix}. \quad (10)$$

Here, we define

$$\begin{aligned}
\mathbf{S} =& \mathbf{I}_N \otimes Df(\mathbf{s}) + \sigma_1 h(0)(r^{(1)} \mathbf{I}_N \otimes Dg^{(1)}) \\
&- 2\sigma_2 (r^{(2)} \mathbf{I}_N \otimes Dg^{(2)}) - \sigma_1 h(0) \mathbf{L}^{(1)} \otimes D_2 g^{(1)} \\
&+ \sigma_2 \mathbf{L}^{(2)} \otimes D_s g^{(2)}\,, \quad (11)
\end{aligned}$$

with $Dg^{(1)} = D_1 g^{(1)} + D_2 g^{(1)}$, $Dg^{(2)} = D_1 g^{(2)} + D_2 g^{(2)} + D_3 g^{(2)}$ and $D_s g^{(2)} = D_2 g^{(2)} + D_3 g^{(2)}$. $\mathbf{I}_N$ is the $N \times N$ identity matrix, $\mathbf{B}^{(1)}$ and $\mathbf{C}^{(1)}$ are suitable constant matrices of order $N \times N^2$ and $N^2 \times N$ (see Appendix B for the explicit form of the latter) that satisfy $\mathbf{B}^{(1)}\mathbf{B}^{(1)^\top} = r^{(1)}\mathbf{I}_N$ and $\mathbf{B}^{(1)}\mathbf{C}^{(1)} = \mathbf{L}^{(1)}$.

Solving the $(N^2 + Nd)$ dimensional variational equation (10) to calculate the Lyapunov exponents provides the necessary condition for the stability of the synchronous solution. The high dimensionality of the variational equation prevents from an analytical study of the latter; however, the structure of the Jacobian matrix in Eq. (10) indicates that there are $(N^2 - N)$ eigenvalues equal to $-\epsilon$, hence $(N^2 - N)$ stable directions with negative Lyapunov exponents, remember that $\epsilon > 0$. The invariant subspace spanned by these eigenvalues allows us to introduce new coordinates, eventually reducing the dimension of (10) by separating the $(N^2 - N)$ stable directions from the remaining $(Nd + N)$ ones. Therefore, the condition for the synchronization can be proved

by studying the remaining $(Nd+N)$ dimensional system. Thereafter, in order to further simplify it and align with the strategy of the Master Stability Equation, we introduce the matrix $\mathbf{U}$ whose columns are the orthonormal eigenvectors of the Laplacian $\mathbf{L}^{(1)}$, i.e., $\mathbf{U}^\top\mathbf{L}^{(1)}\mathbf{U} = \text{diag}\{0=\mu_1^{(1)},\mu_2^{(1)},\dots,\mu_N^{(1)}\}$. Then, we can perform the change of variables

$$\begin{pmatrix} \mathbf{U}\otimes\mathbf{I}_d & 0 \\ 0 & \mathbf{U}\end{pmatrix}\begin{pmatrix}\boldsymbol{\xi}\\ \boldsymbol{\chi}\end{pmatrix} = \begin{pmatrix}\boldsymbol{\zeta}\\ \boldsymbol{\eta}\end{pmatrix},$$

and obtain, after some straightforward but lengthy computation that we postpone to the Appendix B, the following master stability equation (MSE):

$$\begin{aligned}
\dot{\zeta}_i &= \Big[Df(\mathbf{s}) + \sigma_1 h(0) r^{(1)} Dg^{(1)} - \sigma_1 h(0)\mu_i^{(1)} D_2 g^{(1)} + \\
&\quad - 2\sigma_2 r^{(2)} Dg^{(2)}\Big]\zeta_i + \sigma_2 \sum_{j=1}^{N} \tilde{L}^2_{ij} D_s g^{(2)} \zeta_j - \sigma_1 g^{(1)}(\mathbf{s},\mathbf{s})\eta_i, \\
\dot{\eta}_i &= -\epsilon\Big[\mu_i^{(1)} Dh(0)\zeta_i + \eta_i\Big], i = 1,2,\dots,N,
\end{aligned} \tag{12}$$

where we introduced the matrix $\tilde{\mathbf{L}}^{(2)} = \mathbf{U}^\top\mathbf{L}^{(2)}\mathbf{U}$. Therefore, the stability problem of the synchronous solution $(\mathbf{s}, k_{ij}^{(s)})$ is reduced to evaluating the maximum Lyapunov exponent of the above (non-autonomous) linear system of ODE (12); let us recall that negativity of the latter implies the existence of a stable synchronous solution. Let us also observe that the MSE is still an $(Nd+N)$ dimensional coupled equation, and unlike the classical master stability approach, it cannot be further decoupled in N equations of dimension $(d+1)$. Still, analogous to the classical master stability approach, we can separate the modes associated to the parallel and the transverse directions. The variables (ζ_1,η_1) correspond to the parallel modes, whereas the variables associated to $i=2,3,\dots,N$ represent the transverse modes. Here, we use the fact that $\mu_1^{(1)}=0$ and $\mathbf{L}^{(2)}$ being a zero row sum matrix, the elements in the first row and column of the matrix $\tilde{\mathbf{L}}^{(2)}$ are zero.

In general, the MSE can not be decoupled any further; there are, however, relevant cases in which one can take some steps further in the analytical understanding of the problem, as we will hereby show. In these scenarios, as in the classical master stability approach, we can decouple the MSE into N equations of dimension $(d+1)$.

1. all-to-all connection topology

We first consider the case where the higher-order Laplacian $\mathbf{L}^{(2)}$ is a scalar multiple of the pairwise Laplacian $\mathbf{L}^{(1)}$, i.e., $\mathbf{L}^{(2)} = \nu\mathbf{L}^{(1)}$ for some $\nu>0$. A straightforward example of this scenario occurs when the oscillators are globally connected to each other. For all-to-all connection involving N nodes, we have $\mathbf{L}^{(2)} = (N-1)\mathbf{L}^{(1)}$. Therefore, in this case Eq. (12) can be simplified and returns for all $i=1,2,\dots,N$

$$\begin{aligned}
\dot{\zeta}_i &= [Df(\mathbf{s}) + \sigma_1 h(0) r^{(1)} Dg^{(1)} - \sigma_1 h(0)\mu_i^{(1)} D_2 g^{(1)} + \\
&-2\sigma_2 r^{(2)} Dg^{(2)} + \nu\mu_i^{(1)} D_s g^{(2)}]\zeta_i - \sigma_1 g^{(1)}(\mathbf{s},\mathbf{s})\eta_i, \\
\dot{\eta}_i &= -\epsilon[\mu_i^{(1)} Dh(0)\zeta_i + \eta_i]\,.
\end{aligned} \tag{13}$$

Since, for the globally coupled topology, $\nu=(N-1)$ and $\mu_i^{(1)} = N$, for all $i=2,3,\dots,N$, to find the stability of the system, we just need to find the maximum Lyapunov exponent (λ_{max}) of the $(d+1)$ dimensional equation

$$\begin{aligned}
\dot{\zeta} &= [Df(\mathbf{s}) + \sigma_1 h(0) r^{(1)} Dg^{(1)} - \sigma_1 h(0)(N-1) D_2 g^{(1)} + \\
&-2\sigma_2 r^{(2)} Dg^{(2)} + N(N-1) D_s g^{(2)}]\zeta - \sigma_1 g^{(1)}(\mathbf{s},\mathbf{s})\eta, \\
\dot{\eta} &= -\epsilon[NDh(0)\zeta + \eta]\,.
\end{aligned} \tag{14}$$

2. Commuting Laplacian matrices

Another interesting case where one can simplify the MSE, is the one where the pairwise and higher-order Laplacians commute each other, i.e., $\mathbf{L}^{(1)}\mathbf{L}^{(2)} = \mathbf{L}^{(2)}\mathbf{L}^{(1)}$. Let us observe that such a scenario can be obtained by assuming the underlying supports to have nonlocal ring-like topology, where each node is connected to k neighboring nodes on the left and k on the right via pairwise or higher-order connections. Under this assumption the matrices $\mathbf{L}^{(1)}$ and $\mathbf{L}^{(2)}$ are circulant matrices and thus they commute. The latter conclusion implies that the matrix $\mathbf{U}$ diagonalizes also $\mathbf{L}^{(2)}$, i.e., $\mathbf{U}^\top\mathbf{L}^{(2)}\mathbf{U} = \text{diag}\{\mu_1^{(2)},\mu_2^{(2)},\dots,\mu_N^{(2)}\}$. Eventually the MSE (12) simplifies into

$$\begin{aligned}
\dot{\zeta}_i &= [Df(\mathbf{s}) + \sigma_1 h(0) r^{(1)} Dg^{(1)} - \sigma_1 h(0)\mu_i^{(1)} D_2 g^{(1)} + \\
&-2\sigma_2 r^{(2)} Dg^{(2)} + \mu_i^{(2)} D_s g^{(2)}]\zeta_i - \sigma_1 g^{(1)}(\mathbf{s},\mathbf{s})\eta_i, \qquad (15)\\
\dot{\eta}_i &= -\epsilon[\mu_i^{(1)} Dh(0)\zeta_i + \eta_i]\,, i = 1,2,\dots,N. \qquad (16)
\end{aligned}$$

Thus, the MSE decouples into N blocks of $(d+1)$-dimensional equations. Solving these low dimensional equations for the calculation of maximum Lyapunov exponent, λ_{max}, provides the necessary conditions for the stability of the synchronous solution. It is important to note that λ_{max} depends only on the coupling strengths and the structural properties of the connection topology, via the eigenvalues and the (generalized) degrees, resembling thus to the classical MSE approach.

B. Numerical Results

Let us now present some numerical results to support the theory presented above. Because we will not make any assumption on the coupling function, in particular, they will not be noninvasive, we recall that the underlying support should satisfy $\sum_{j=1}^{N} a_{ij}^{(1)} = r^{(1)}$ and

$\sum_{j=1}^{N}\sum_{p=1}^{N} a_{ijp}^{(2)} = 2r^{(2)}$, for all i, for the synchronous solution to exist. To perform the numerical simulations, we integrate the adaptive higher-order system using the fourth-order Runge-Kutta (RK4) algorithm with adaptive time-stepping, maintaining a relative tolerance of 10^{-8} for $T = 10^4$ time units and unless stated otherwise, the number of oscillators is set fixed to $N = 200$.

1. *Kuramoto oscillators with all-to-all topology*

The first example we propose is a Kuramoto model with pairwise and three-body interactions and phase lags [19, 67] defined via an all-to-all coupling. The system's

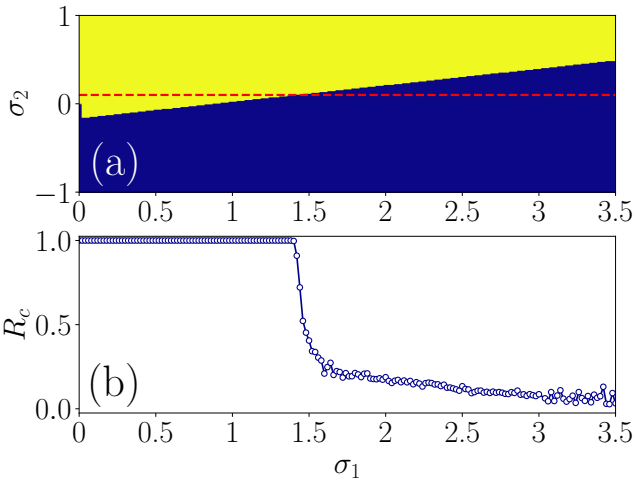

FIG. 1. (a) Phase diagram in the $\sigma_1 - \sigma_2$ plane illustrating synchronization in the Kuramoto model with lag and all-to-all coupling (model I). Regions associated with positive Lyapunov exponents are colored blue (dark) and thus correspond to absence of synchronization, while yellow (bright) zones indicate negative MSF returning parameters values for which the system synchronizes. (b) The order parameter R_c is plotted as a function of σ_1 for $\sigma_2 = 0.1$, starting from the synchronization state with initial conditions close to $\theta_i(0) = 0$ and $k_{ij}^{(1)} = -a_{ij}^{(1)}\sin(\beta_1)$ indicated by the horizontal red-dashed line in (a). It is observed that the MSF becomes positive precisely at the value of σ_1 where $R_c < 1$, signifying a decrease from synchrony. Other parameters are $N = 200$, $\alpha_1 = \alpha_2 = 0.49\pi$, $\beta_1 = 0.88\pi$, $\epsilon_1 = 0.01$. The order parameterR_c is calculated by averaging over the last 25% of the integration interval and by performing 20 realizations.

state is thus described by N angular variables, θ_i, and N^2 links weights; we recall that we are still assuming the three-body interaction to not evolve and thus be fixed to 1. In equations,

$$\dot{\theta}_i = \omega - \frac{\sigma_1}{N}\sum_{j=1}^{N} a_{ij}^{(1)} k_{ij}^{(1)} \sin(\theta_i - \theta_j + \alpha_1) + - \frac{\sigma_2}{N^2}\sum_{j=1}^{N}\sum_{p=1}^{N} a_{ijp}^{(2)} \sin(2\theta_i - \theta_j - \theta_p + \alpha_2), \quad (17)$$

$$\dot{k}_{ij}^{(1)} = -\epsilon_1[k_{ij}^{(1)} + a_{ij}^{(1)} \sin(\theta_i - \theta_j + \beta_1)]\,, \quad (18)$$

where $\alpha_1 > 0$ (resp. α_2) determines the pairwise (resp. three-body) lag, while β_1 is the lag in the evolution of links weights. To allow for a global synchronous solution we assume the proper frequency to be equal each other and without any loss of generality, we consider $\omega = 0$ here and throughout the rest of the manuscript by choosing a suitable frame of reference.

The global synchronous solution is given by

$$\mathbf{s}(t) = \left(\frac{\sigma_1}{N} r^{(1)} \sin\alpha_1 \sin\beta_1 - \frac{\sigma_2}{N^2} 2r^{(2)} \sin\alpha_2\right) t, \quad (19)$$

$$k_{ij}^{(s)} = -a_{ij}^{(1)} \sin\beta_1\,, \quad (20)$$

whose stability can be studied by using Eq. (14), namely

$$\begin{bmatrix}\dot{\zeta}\\ \dot{\eta}\end{bmatrix} = \begin{bmatrix}M_{11} & M_{12}\\ M_{21} & M_{22}\end{bmatrix}\begin{bmatrix}\zeta\\ \eta\end{bmatrix}, \quad (21)$$

where

$$M_{11} = \sigma_1 \cos\alpha_1 \sin\beta_1 - 2\frac{\sigma_2}{N}(N-1)\cos\alpha_2,$$
$$M_{12} = -\frac{\sigma_1}{N}\sin\alpha_1,\ M_{21} = -\epsilon_1 N \cos\beta_1 \text{ and } M_{22} = -\epsilon_1\,.$$

The characteristic polynomial of the latter system is

$$\lambda^2 + \lambda\left(\epsilon_1 - \sigma_1\cos\alpha_1\sin\beta_1 + 2\frac{\sigma_2}{N}(N-1)\cos\alpha_2\right) - \epsilon_1\left(\sigma_1\sin(\alpha_1+\beta_1) - 2\frac{\sigma_2}{N}(N-1)\cos\alpha_2\right) = 0\,, \quad (22)$$

whose roots can be straightforwardly computed, and thus, the stability of the synchronous solution can be inferred. The results are reported in Fig. 1 (a), where we show the synchronization region as a function of the coupling parameters σ_1 and σ_2 by using a color code: yellow $\max(\mathrm{Re}\,\lambda) < 0$ and blue otherwise. It can be observed that for $\sigma_2 \geq 0$, the system goes through a transition from synchronization to desynchronization until a critical value of $\sigma_2 \approx 0.58$. Beyond this, the system always remains in synchrony. On the other hand, for $\sigma_2 < 0$, up to a small range of σ_2 (≈ -0.15), a bounded region of synchronization can be observed, i.e., at first a transition from desynchrony to synchrony is observed within a small window of σ_1, and then synchrony to desynchrony emerges. Beyond this, the system never settles in a stable synchronous solution.

To perform numerical investigations, we utilize the cluster order parameter R_c [19, 68, 69] to measure the system coherence. R_c is given by the number of pairwise coherent oscillators normalized by the total number of pairs N^2. Mathematically, it is defined as,

$$R_c = \frac{1}{N^2}\sum_{i,j=1}^{N} R_{ij}\,, \tag{23}$$

where

$$R_{ij} = \left|\frac{1}{\Delta t}\int_{T-\Delta t}^{T} \exp\{\mathrm{i}[\theta_i(t)-\theta_j(t)]\}dt\right|. \tag{24}$$

Thus, in an incoherent (resp. fully coherent) state, R_c returns the values 0 (reps. 1). While for the frequency cluster states, it takes the value $0 < R_c < 1$. Figure 1(b) portrays the variation of R_c as a function of σ_1 for a fixed higher-order coupling, $\sigma_2 = 0.1$; the system has been intialized starting from the synchronization state with initial conditions close to $\theta_i(0) = 0$ and $k_{ij}^{(1)} = -a_{ij}^{(1)}\sin(\beta_1)$. We can observe the existence of a transition from full synchronization to desynchronization through intermediate cluster states (decreasing R_c), which shows good agreement with the analytical findings.

Let us now consider a slightly different higher-order Kuramoto model still involving pairwise and three-body interactions defined through all-to-all coupling topology. In this case, the chosen higher-order interaction term has an asymmetric form, similar to those recently used by several researchers [45]. The dynamics of the system is given by

$$\begin{aligned}\dot{\theta}_i =&\omega - \frac{\sigma_1}{N}\sum_{j=1}^{N} a_{ij}^{(1)}k_{ij}^{(1)}\sin(\theta_i-\theta_j+\alpha_1)+\\ &-\frac{\sigma_2}{N^2}\sum_{j=1}^{N}\sum_{p=1}^{N} a_{ijp}^{(2)}\sin(2\theta_j-\theta_p-\theta_i+\alpha_2),\end{aligned} \tag{25}$$

$$\dot{k}_{ij}^{(1)} = -\epsilon_1[k_{ij}^{(1)} + a_{ij}^{(1)}\sin(\theta_i-\theta_j+\beta_1)]\,. \tag{26}$$

The synchronous solution is

$$\mathbf{s}(t) = \left(\frac{\sigma_1}{N}r^{(1)}\sin\alpha_1\sin\beta_1 - \frac{\sigma_2}{N^2}2r^{(2)}\sin\alpha_2\right)t, \tag{27}$$

$$k_{ij}^{(s)} = -a_{ij}^{(1)}\sin\beta_1\,, \tag{28}$$

whose stability can be studied by applying strategy similar to the one used above and thus returning the linear system

$$\begin{bmatrix}\dot{\zeta}\\ \dot{\eta}\end{bmatrix} = \begin{bmatrix}M_{11} & M_{12}\\ M_{21} & M_{22}\end{bmatrix}\begin{bmatrix}\zeta\\ \eta\end{bmatrix}, \tag{29}$$

where

$$M_{11} = \sigma_1\cos\alpha_1\sin\beta_1 + \frac{\sigma_2}{N}(N-1)\cos\alpha_2,$$

$$M_{12} = -\frac{\sigma_1}{N}\sin\alpha_1,\ M_{21} = -\epsilon_1 N\cos\beta_1 \text{ and } M_{22} = -\epsilon_1.$$

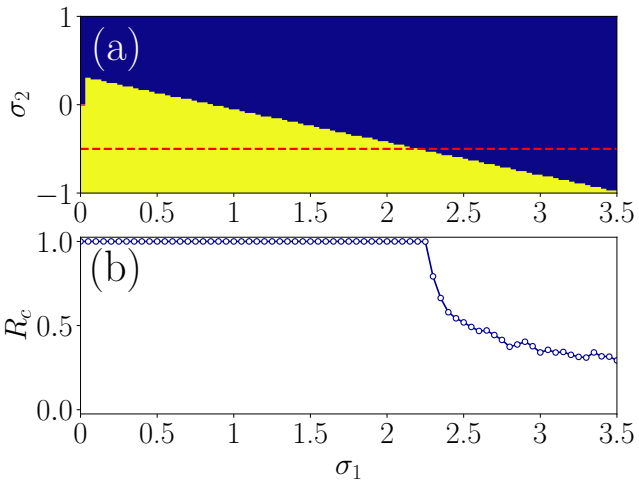

FIG. 2. (a) Phase diagram of the MSF in the $\sigma_1 - \sigma_2$ plane (coupling parameters), illustrating synchronization behavior in the Kuramoto model with lag and all-to-all coupling (Model II). In the diagram, regions with positive Lyapunov exponents are shown in blue (dark), indicating instability and thus desynchronization, while yellow (bright) zones represent regions of negative MSF, corresponding to stability, hence to a stable synchronous state. (b) The order parameter R_c is shown as a function of σ_1 for $\sigma_2 = -0.5$ by starting from the synchronization state with initial conditions close to $\theta_i(0) = 0$ and $k_{ij}^{(1)} = -a_{ij}^{(1)}\sin(\beta_1)$ corresponding to the horizontal red-dashed line in (a). The MSF is observed to become positive precisely at the σ_1 value where $R_c < 1$, signifying a decrease from synchrony. Other model parameters are kept the same as in Fig. 1.

The corresponding characteristics polynomial to the above linear system is

$$\begin{aligned}&\lambda^2 + \left(\epsilon_1 - \sigma_1\cos\alpha_1\sin\beta_1 - \frac{\sigma_2}{N}(N-1)\cos\alpha_2\right)\lambda\\ &-\epsilon_1\left(\sigma_1\sin(\alpha_1+\beta_1) + \frac{\sigma_2}{N}(N-1)\cos\alpha_2\right) = 0\,.\end{aligned} \tag{30}$$

In Fig. 2 we report the MSF [Fig. 2(a)] computed again as a function of σ_1 and σ_2 and compared with the order parameter R_c [Fig. 2(b)]. Here, we can observe a relatively opposite scenario as compared to the results of the first model. It can be remarked that for $\sigma_2 \leq 0$, the system goes through a transition from synchronization to desynchronization until a critical value of $\sigma_2 \approx -0.97$ is reached. Beyond this value, the system always remains synchronized. On the other hand, for $\sigma_2 > 0$, up to a small range of $\sigma_2(\approx 0.3)$, a bounded region of synchronization can be observed, beyond which the system never settles in a stable synchronous solution.

2. *Kuramoto oscillators with nonlocal connection topology*

To move forward, we again consider the higher-order Kuramoto model, given by Eqs. (17) and (18) but with

the pairwise and higher-order coupling realized via a nonlocal connection topology. More precisely, the oscillators are connected through a ring-like topology where each node is connected to $k = 30$ neighboring nodes on the left and $k = 30$ on the right via pairwise connections. The associated triadic connections are formed by promoting all the triangles composed of three different pairwise links. In this way, the oscillators can engage in both pairwise interactions, when connected by a network link, and three-body interactions, when they are part of the same triangle. By following Eqs. (15) and (16), the stability of the synchronous solution can be inferred by solving the roots of the characteristics equation corresponding to each one of the $(N-1)$ blocks (since the first block is associated with the parallel modes). The characteristics equation for each block $i = 2, 3, \ldots, N$ is given by,

$$\lambda_i^2 + \lambda_i \left(\epsilon_1 - \frac{\sigma_1}{N}\mu_i^{(1)} \cos\alpha_1 \sin\beta_1 + 2\frac{\sigma_2}{N^2}\mu_i^{(2)} \cos\alpha_2\right) - \epsilon_1 \mu_i^{(1)} \left(\frac{\sigma_1}{N}\sin(\alpha_1+\beta_1) - 2\frac{\sigma_2}{N^2}(N-1)\cos\alpha_2\right) = 0\,. \tag{31}$$

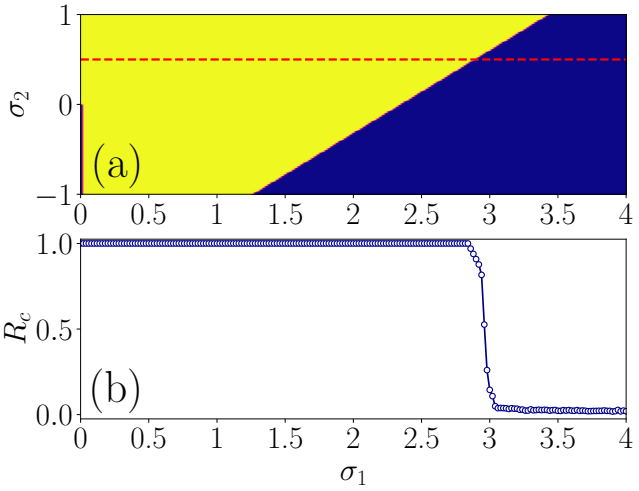

FIG. 3. (a) Phase diagram of the MSF in the $\sigma_1 - \sigma_2$ plane (coupling parameters) illustrating synchronization in the Kuramoto model with lag and nonlocal coupling topology. Regions with positive Lyapunov exponents are colored blue (dark) and are thus associated to an unstable synchronous state, while yellow (bright) zones indicate negative MSF to which one can associate synchronization. (b) Plot of the order parameter R_c as a function of σ_1 for $\sigma_2 = 0.5$ starting from the synchronization state with initial conditions close to $\theta_i(0) = 0$ and $k_{ij}^{(1)} = -a_{ij}^{(1)} \sin(\beta_1)$, as represented by the horizontal red-dashed line in (a). The remaining model parameters are kept constant as in Fig. 1, with the number of connected oscillators on both sides set to $k = 30$.

A negative value of $\lambda_{max} = \max\{\mathrm{Re}\,\lambda_i\}$ signifies the emergence of stable synchronous solution. Results are reported in Fig. 3 where λ_{max} (panel (a)) is computed as a function of σ_1 and σ_2 and compared with the order parameter R_c (panel (b)) for a fixed σ_2. It can be observed that the system goes through a transition from full synchronization to desynchronization with increasing σ_1 for $\sigma_2 \geq 0$. On the other hand, for $\sigma_2 < 0$, the system achieves synchronization in a bounded region. It is also worth noticing that with increasing σ_2 from negative to positive, the synchronization region becomes much wider.

III. ADAPTIVE PAIRWISE AND HIGHER-ORDER INTERACTIONS

The aim of this section is to generalize the previous study by relaxing the assumption about the static higher-order interactions; more precisely, we now assume the pairwise weights and the higher-order ones to evolve as functions of the system state. More precisely, by restricting again, for the sake of pedagogy, our analysis to the three-body interaction, we are considering the model

$$\dot{\mathbf{x}}_i = f(\mathbf{x}_i) - \sigma_1 \sum_{j=1}^{N} a_{ij}^{(1)} k_{ij}^{(1)}(t) g^{(1)}(\mathbf{x}_i, \mathbf{x}_j) + - \sigma_2 \sum_{j=1}^{N}\sum_{p=1}^{N} a_{ijp}^{(2)} k_{ijp}^{(2)}(t) g^{(2)}(\mathbf{x}_i, \mathbf{x}_j, \mathbf{x}_p)\,, \tag{32}$$

where $g^{(1)}(\mathbf{x}_i, \mathbf{x}_j)$ and $g^{(2)}(\mathbf{x}_i, \mathbf{x}_j, \mathbf{x}_k)$ are the coupling functions, and the weights of pairwise, $k_{ij}^{(1)}$, and three-body interactions, $k_{ijp}^{(2)}$, evolve as follows

$$\dot{k}_{ij}^{(1)} = -\epsilon_1 [k_{ij}^{(1)} + a_{ij}^{(1)} h^{(1)}(\mathbf{x}_i - \mathbf{x}_j)], \tag{33}$$

$$\dot{k}_{ijp}^{(2)} = -\epsilon_2 [k_{ijp}^{(2)} + a_{ijp}^{(2)} h^{(2)}(2\mathbf{x}_i - \mathbf{x}_j - \mathbf{x}_p)]\,. \tag{34}$$

Here, $h^{(1)}$ and $h^{(2)}$ denote adaptation functions. ϵ_i, $i = 1, 2$ is the time scale separation parameter, which is generally taken to be a very small positive real number.

The global synchronous solution of the above adaptive model is given by $(\mathbf{s}, k_{ij}^{(s)}, k_{ijk}^{(s)})$ and it satisfies

$$\dot{\mathbf{s}} = f(\mathbf{s}) + \sigma_1 r^{(1)} h^{(1)}(0) g^{(1)}(\mathbf{s}, \mathbf{s}) + 2\sigma_2 r^{(2)} h^{(2)}(0) g^{(2)}(\mathbf{s}, \mathbf{s}, \mathbf{s}), \tag{35}$$

$$k_{ij}^{(s)} = -a_{ij}^{(1)} h^{(1)}(0), \tag{36}$$

$$k_{ijp}^{(s)} = -a_{ijp}^{(2)} h^{(2)}(0)\,. \tag{37}$$

It is important to note that here, once again, we have not imposed any conditions on the coupling functions, and thus, the underlying connectivity has constant (generalized) degrees $r^{(i)}$, $i = 1, 2$. The analysis with non-invasive coupling functions is illustrated in Appendix A.

A linear stability analysis about this solution can be performed to infer the existence of a stable synchronous solution. We thus perturb the system with small perturbation terms $\xi_i = \mathbf{x}_i - \mathbf{s}$, $\chi_{ij} = k_{ij}^{(1)} - k_{ij}^{(s)}$ and $\eta_{ijp} = k_{ijp}^{(2)} - k_{ijp}^{(s)}$, and we study their time evolution via the variational equations,

$$
\begin{aligned}
\dot{\xi}_i =& Df(\mathbf{s})\xi_i + \sigma_1 r^{(1)} h^{(1)}(0) Dg^{(1)}(\mathbf{s},\mathbf{s})\xi_i + 2\sigma_2 r^{(2)} h^{(2)}(0) Dg^{(2)}(\mathbf{s},\mathbf{s},\mathbf{s})\xi_i - \sigma_1 h^{(1)}(0) \sum_{j=1}^{N} L_{ij}^{(1)} D_2 g^{(1)}(\mathbf{s},\mathbf{s})\xi_j + \\
& - \sigma_2 h^{(2)}(0) \sum_{j=1}^{N} L_{ij}^{(2)} D_s g^{(2)}(\mathbf{s},\mathbf{s},\mathbf{s})\xi_j - \sigma_1 \sum_{j=1}^{N} a_{ij}^{(1)} \chi_{ij} g^{(1)}(\mathbf{s},\mathbf{s}) - \sigma_2 \sum_{j=1}^{N}\sum_{p=1}^{N} a_{ijp}^{(2)} \eta_{ijp} g^{(2)}(\mathbf{s},\mathbf{s},\mathbf{s}), \\
\dot{\chi}_{ij} =& -\epsilon_1(\chi_{ij} + a_{ij}^{(1)} Dh^{(1)}(0)(\xi_i - \xi_j)), \\
\dot{\eta}_{ijp} =& -\epsilon_2(\eta_{ijp} + a_{ijp}^{(2)} Dh^{(2)}(0)(2\xi_i - \xi_j - \xi_p)),
\end{aligned} \tag{38}
$$

which is a $(N^3 + N^2 + Nd)$-dimensional coupled linear differential equation. In matrix form, the above variational equations can be written as

$$
\begin{bmatrix} \dot{\boldsymbol{\xi}} \\ \dot{\boldsymbol{\chi}} \\ \dot{\boldsymbol{\eta}} \end{bmatrix} = \begin{bmatrix} \mathbf{S}_2 & -\sigma_1 \mathbf{B}^{(1)} \otimes g^{(1)}(\mathbf{s},\mathbf{s}) & -\sigma_2 \mathbf{B}^{(2)} \otimes g^{(2)}(\mathbf{s},\mathbf{s},\mathbf{s}) \\ -\epsilon_1 \mathbf{C}^{(1)} \otimes Dh^{(1)}(0) & -\epsilon_1 \mathbf{I}_{N^2} & 0 \\ -\epsilon_2 \mathbf{C}^{(2)} \otimes Dh^{(2)}(0) & 0 & -\epsilon_2 \mathbf{I}_{N^3} \end{bmatrix} \begin{bmatrix} \boldsymbol{\xi} \\ \boldsymbol{\chi} \\ \boldsymbol{\eta} \end{bmatrix}, \tag{39}
$$

where we consider again the matrix $\boldsymbol{\chi}$, resp. the tensor $\boldsymbol{\eta}$, as N^2, resp. N^3, columns vectors by stacking the rows over rows similarly to the previous case, and we introduced suitable matrices

$$
\begin{aligned}
\mathbf{S}_2 =& \mathbf{I}_N \otimes Df(\mathbf{s}) + \sigma_1 h^{(1)}(0)(r^{(1)}\mathbf{I}_N \otimes Dg^{(1)}) \\
& + 2\sigma_2 h^{(1)}(0)(r^{(2)}\mathbf{I}_N \otimes Dg^{(2)}) - \sigma_1 h^{(1)}(0)\mathbf{L}^{(1)} \otimes D_2 g^{(1)} \\
& - \sigma_2 h^{(2)}(0)\mathbf{L}^{(2)} \otimes D_s g^{(2)},
\end{aligned} \tag{40}
$$

$\mathbf{B}^{(1)}$ and $\mathbf{C}^{(1)}$ are the same constant matrices of order $N \times N^2$ and $N^2 \times N$ used in Section II, while $\mathbf{B}^{(2)}$ and $\mathbf{C}^{(2)}$ are constant matrices of order $N \times N^3$ and $N^3 \times N$, satisfying $\mathbf{B}^{(2)}\mathbf{B}^{(2)^\top} = 2r^{(2)}\mathbf{I}_N$ and $\mathbf{B}^{(2)}\mathbf{C}^{(2)} = \mathbf{L}^{(2)}$ (we refer the interested reader to Appendix B for a longer description of the derivation of those matrices).

It is important to note that an analytical stability condition for the synchronization solution can be derived for arbitrary ϵ_1 and ϵ_2. However, in such case, one must deal with the very large $(N^3 + N^2 + Nd)$-dimensional coupled variational equation (38) or (39) to compute the maximum Lyapunov exponent. Moreover, this high-dimensional system cannot generally be decoupled into lower-dimensional equations, making the analysis significantly more challenging. Thus, to move forward in reducing the dimension of the higher dimensional variational equation (38) and to be able to get clear analytical insight, hereafter we assume $\epsilon_1 = \epsilon_2 = \epsilon$. Let us also observe that one can relax the above assumption by considering noninvasive coupling functions $g^{(1)}$ and $g^{(2)}$ (see Appendix A). Leaving the details of the computation to the Appendix B, we can eventually obtain the $(Nd + 2N)$-dimensional MSE ruling the evolution of the perturbations

$$
\begin{aligned}
\dot{\hat{\xi}}_i =& \Big[Df(\mathbf{s}) + \sigma_1 h^{(1)}(0) r^{(1)} Dg^{(1)} \\
& + 2\sigma_2 r^{(2)} h^{(2)}(0) Dg^{(2)} - \sigma_1 h^{(1)}(0) \mu_i^{(1)} D_2 g^{(1)} \Big] \hat{\xi}_i \\
& - \sigma_2 h^{(2)}(0) \sum_{j=1}^{N} \tilde{L}_{ij}^2 D_s g^{(2)} \hat{\xi}_j - \sigma_1 g^{(1)}(s,s)\hat{\chi}_i \\
& - \sigma_2 g^{(2)}(s,s,s)\hat{\eta}_i, \\
\dot{\hat{\chi}}_i =& -\epsilon[\mu_i^{(1)} Dh^{(1)}(0)\hat{\xi}_i + \hat{\chi}_i], \\
\dot{\hat{\eta}}_i =& -\epsilon[\sum_{j=1}^{N} \tilde{L}_{ij}^2 Dh^{(2)}(0)\hat{\xi}_j + \hat{\eta}_i],
\end{aligned} \tag{41}
$$

where we introduced new coordinates $(\hat{\boldsymbol{\xi}}, \hat{\boldsymbol{\chi}}, \hat{\boldsymbol{\eta}})^\top$ related to the previous ones by

$$
\begin{pmatrix} \mathbf{U} \otimes \mathbf{I}_d & 0 & 0 \\ 0 & \mathbf{U} & 0 \\ 0 & 0 & \mathbf{U} \end{pmatrix} \begin{pmatrix} \boldsymbol{\xi} \\ \boldsymbol{\chi} \\ \boldsymbol{\eta} \end{pmatrix} = \begin{pmatrix} \hat{\boldsymbol{\xi}} \\ \hat{\boldsymbol{\chi}} \\ \hat{\boldsymbol{\eta}} \end{pmatrix},
$$

with $\mathbf{U}$ the matrix whose columns are the orthonormal eigenvectors that diagonalizes the pairwise Laplacian $\mathbf{L}^{(1)}$, i.e., $\mathbf{U}^\top \mathbf{L}^{(1)} \mathbf{U} = \mathrm{diag}\{\mu_1^{(1)}, \mu_2^{(1)}, \ldots, \mu_N^{(1)}\}$ and $\tilde{\mathbf{L}}^{(2)} = \mathbf{U}^\top \mathbf{L}^{(1)} \mathbf{U}$.

Therefore, the stability problem of the synchronous solution is reduced to evaluating the maximum Lyapunov exponent of the above coupled linear differential equation (41). Once again, we are faced with the problem that, in general, the MSE (41) can not be decoupled further. Still, analogous to the classical master stability approach [64, 65], we can separate the modes associated with parallel and transverse directions. The variables $(\hat{\xi}_1, \hat{\chi}_1, \hat{\eta}_1)$ correspond to the parallel models, whereas the variables associated with $i = 2, 3, \ldots, N$ represent the transverse modes. Here, we once again use the fact that $\mu_1^{(1)} = 0$

and $\mathbf{L}^{(2)}$ being a zero row sum matrix, the elements in the first row and column of the matrix $\tilde{\mathbf{L}}^{(2)}$ are zero. In general, the transverse modes of the MSE (41) can not be further separated. However, there are interesting cases in which the MSE can be fully decoupled, similar to what has been addressed for the only pairwise adaptation case, i.e., when the higher-order Laplace matrix is a scalar multiple of the pairwise one and the scenario of commuting Laplacian matrices. In these cases, thus, the MSE can be separated into N $(d+2)$-dimensional equations, and the maximum Lyapunov exponents depend only on the interaction coupling strengths and the underlying structure properties via the eigenvalues of the Laplace matrices and the (generalized) degrees.

For the all-to-all coupling configuration similar to the only pairwise adaptation case, the MSE reduced into $(d+2)$-dimensional equations given by

$$\begin{aligned}
\dot{\hat{\xi}} =& \Big[Df(\mathbf{s}) + \sigma_1 h^{(1)}(0) r^{(1)} Dg^{(1)} \\
&+ 2\sigma_2 r^{(2)} h^{(2)}(0) Dg^{(2)} - \sigma_1 h^{(1)}(0) \mu^{(1)} D_2 g^{(1)}\Big] \hat{\xi} \\
&- \sigma_2 h^{(2)}(0) \nu \mu^{(1)} D_s g^{(2)} \hat{\xi} - \sigma_1 g^{(1)}(s,s) \hat{\chi} \\
&- \sigma_2 g^{(2)}(s,s,s) \hat{\eta}, \\
\dot{\hat{\chi}} =& -\epsilon[\mu^{(1)} Dh^{(1)}(0) \hat{\xi} + \hat{\chi}], \\
\dot{\hat{\eta}} =& -\epsilon[\nu \mu^{(1)} Dh^{(2)}(0) \hat{\xi} + \hat{\eta}], \qquad (42)
\end{aligned}$$

where $\nu = N-1$ and $\mu^{(1)} = N$. Thus, the problem of stability analysis is reduced to solve the $(d+2)$-dimensional equation for the calculation of the maximum Lyapunov exponent.

For the nonlocal ring like topology (i.e., where the pairwise and higher-order Laplacians commute each other), following the similar procedure as in the case of only pairwise adaptation, the MSE reduced into N blocks of $(d+2)$-dimensional equations given by

$$\begin{aligned}
\dot{\hat{\xi}}_i =& \Big[Df(\mathbf{s}) + \sigma_1 h^{(1)}(0) r^{(1)} Dg^{(1)} \\
&+ 2\sigma_2 r^{(2)} h^{(2)}(0) Dg^{(2)} - \sigma_1 h^{(1)}(0) \mu_i^{(1)} D_2 g^{(1)}\Big] \hat{\xi}_i \\
&- \sigma_2 h^{(2)}(0) \mu_i^{(2)} D_s g^{(2)} \hat{\xi}_i - \sigma_1 g^{(1)}(s,s) \hat{\chi}_i \\
&- \sigma_2 g^{(2)}(s,s,s) \hat{\eta}_i, \\
\dot{\hat{\chi}}_i =& -\epsilon[\mu_i^{(1)} Dh^{(1)}(0) \hat{\xi}_i + \hat{\chi}_i], \\
\dot{\hat{\eta}}_i =& -\epsilon[\mu_i^{(2)} Dh^{(2)}(0) \hat{\xi}_i + \hat{\eta}_i], \; i = 1, 2, \ldots, N, \qquad (43)
\end{aligned}$$

where $\mu_i^{(1)}$ and $\mu_i^{(2)}$ are the eigenvalues of the pairwise and higher-order Laplacian matrices, respectively. The first block of the system of equations, corresponding to $i = 1$, is associated with the modes that are parallel to the synchronization manifold. The remaining $N-1$ blocks correspond to the modes that are transverse to the synchronization solution. Therefore, the stability analysis can be reduced to solving these $N-1$ blocks of $(d+2)$-dimensional equations in order to compute the maximum Lyapunov exponent.

A. Numerical Analysis

The above presented theory will be illustrated by using the adaptive higher-order Kuramoto oscillators with a lag whose equations of motions are given for all $i, j, p \in \{1, 2, \ldots, N\}$ by

$$\begin{aligned}
\dot{\theta}_i =& \omega - \frac{\sigma_1}{N} \sum_{j=1}^{N} a_{ij}^{(1)} k_{ij}^{(1)} \sin(\theta_i - \theta_j + \alpha_1) \\
&- \frac{\sigma_2}{N^2} \sum_{j=1}^{N} \sum_{p=1}^{N} a_{ijp}^{(2)} k_{ijp}^{(2)} \sin(2\theta_i - \theta_j - \theta_p + \alpha_2), \\
\dot{k}_{ij}^{(1)} =& -\epsilon_1 [k_{ij}^{(1)} + a_{ij}^{(1)} \sin(\theta_i - \theta_j + \beta_1)], \\
\dot{k}_{ijp}^{(2)} =& -\epsilon_2 \left[k_{ijp}^{(2)} + a_{ijp}^{(2)} \sin(2\theta_i - \theta_j - \theta_p + \beta_2)\right]. \qquad (44)
\end{aligned}$$

As examples in which the MSE can be further simplified, we consider again the case of globally connected and nonlocal ring like networks. We fixed the number of nodes to $N = 200$, the lag parameters $\alpha_1 = 0.49\pi$, $\beta_1 = 0.88\pi$, $\alpha_2 = 0.49\pi$ and we consider three values $\beta_2 \in \{0.5\pi, 0.88\pi, 1.2\pi\}$. Then, for each value of the latter, we compute the order parameter R_c starting from the synchronous state (i.e., $\theta_i(0) = 0$, $k_{ij}^{(1)} = -a_{ij}^{(1)} \sin\beta_1$ and $k_{ijp}^{(2)} = -a_{ijp}^{(2)} \sin\beta_2$) in the (σ_1, σ_2) parameter space where $\sigma_1 \in [0, 4]$ and $\sigma_2 \in [-1, 1]$.

1. *All-to-all topology*

The results with all-to-all network topology are reported in Fig. 4 where we show (top panels (a)-(c)) the order parameter as a function of σ_1 and σ_2 and we compare it with the analytical prediction obtained by solving the MSE, given by Eq. (42) (bottom panels (d)-(f)). We can observe an excellent agreement between the two methods indeed in both cases, $R_c \ll 1$ and $\max(\mathrm{Re}\,\lambda) > 0$ (blue areas), testifying the absence of synchronization, do (almost) coincide.

Let us now observe that the higher-order adaptation coupling β_2 in Fig. 4 is chosen in such a way that it satisfies the relations $\beta_2 < \beta_1$, $\beta_2 = \beta_1$, and $\beta_2 > \beta_1$, respectively, while all the other parameter values are kept fixed as in Fig. 1 where only the pairwise adaptation is active. We select these values of β_2 to investigate how, depending on the choice of β_2, the stability region is affected by higher-order adaptation, in contrast to constant higher-order interactions. We observe a relatively opposite scenario in the case of $\beta_2 < \beta_1$ as compared to the result of Fig. 1. The system never settles into the stable synchronization state for larger values of $\sigma_2 > 0$, while for larger negative values of σ_2, the system always remains in the synchronized solution [see Fig. 4 (a), (d)]. For the intermediate values of σ_2, a transition from synchrony to desynchrony emerges with increasing value of σ_1. Figures 4 (b) and 4 (e) portray the result for $\beta_2 = \beta_1$. Here,

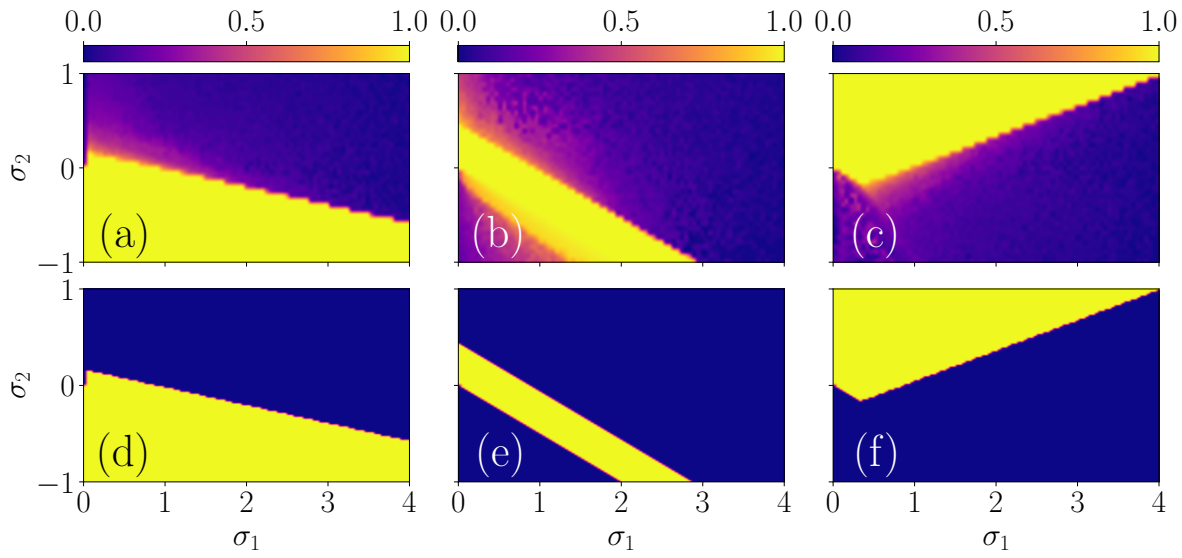

FIG. 4. Globally connected Kuramoto oscillators with both pairwise and higher-order adaptations. Phase diagrams in the $\sigma_1 - \sigma_2$ plane depict the order parameter starting from a synchronization state with initial conditions close to $\theta_i(0) = 0$, $k_{ij}^{(1)} = -a_{ij}^{(1)} \sin\beta_1$ and $k_{ijp}^{(2)} = -a_{ijp}^{(2)} \sin\beta_2$, for three values of β_2: (a) $\beta_2 = 0.5\pi$, (b) $\beta_2 = 0.88\pi$, and (c) $\beta_2 = 1.2\pi$ for the case of adaptive higher-order Kuramoto model with lag and an all-to-all coupling. Panels (d)-(f) display the MSF for the adaptive Kuramoto model, wherein the regions with positive MLE are colored blue (dark) and correspond to desynchronization, while those with negative MLE are yellow (bright) for which the system exhibits synchronization. It is observed that the MSF is positive precisely where the order parameter R_c deviates from synchrony, i.e., $R_c = 1$ The remaining parameters were set to $N = 200$, $\alpha_1 = \alpha_2 = 0.49\pi$, $\beta_1 = 0.88\pi$, $\epsilon_1 = \epsilon_2 = 0.01$.

we observe that for negative values of σ_2, the system went through a double transition with increasing σ_1, i.e., at first desynchrony to synchrony and then synchrony to desynchrony. Therefore, a significantly large bounded region of stable synchronous solution is observed. While for $\sigma_2 \geq 0$, a transition from synchrony to desynchrony emerges up to $\sigma_2 \approx 0.42$, beyond which the system never settles into the stable synchronous solution. Lastly, the results for $\beta_2 > \beta_1$ are illustrated through Figs. 4 (c) and 4 (f), respectively. In this case, the system exhibits qualitatively similar behavior as in the case of no higher-order adaptation, but the region of the stable synchronized state becomes wider.

Therefore, the introduction of higher-order adaptation leads to significantly different qualitative behaviors compared to the case without it. Depending on the choice of higher-order adaptation coupling, synchronization may emerge, be enhanced, weakened, or even completely suppressed.

2. *Nonlocal connection topology*

We now move forward to the next scenario, where the Kuramoto oscillators interact through a nonlocal connection topology. Similar to the case involving only pairwise adaptation (Sec. II), we again consider that the oscillators are connected through a ring-like topology where each node is connected to $k = 30$ neighboring nodes on the left and $k = 30$ on the right via pairwise connections. The associated triadic connections are formed by promoting all the triangles composed of three different pairwise links. In this way, the oscillators can engage in both pairwise interactions, when connected by a network link, and three-body interactions, when they are part of the same triangle. The corresponding results are presented in Fig. 5. The top panels (Fig. 5(a-c)) show the order parameter R_c as a function of σ_1 and σ_2, and these results are compared with the analytical predictions obtained by solving the MSE (43) in the bottom panels (Fig. 5(d-f)). We observe excellent agreement between the numerical and analytical findings. In both cases, regions where $R_c \ll 1$ and max(Re λ)>0 (blue areas), indicating the absence of synchronization, almost perfectly overlap.

Let us once again note that by incorporating higher-order adaptations (Fig.5), we qualitatively alter the stability region of the synchronization solution compared to the case with constant higher-order interactions (Fig.3), depending on the choice of higher-order adaptive coupling strength β_2. Similar to the all-to-all connection topology, here too, for $\beta_2 < \beta_1$, we observe a contrasting scenario compared to the case with only pairwise adaptation. Notably, when $\beta_2 < \beta_1$, as σ_2 decreases from positive to negative, the synchronization region widens significantly [Fig.5(a,d)], which is qualitatively opposite to the result shown in Fig.3(a). For $\beta_2 = \beta_1$, a clearly defined bounded synchronization region emerges when the higher-order coupling is repulsive (i.e., σ_2) [Fig.5(b,e)].

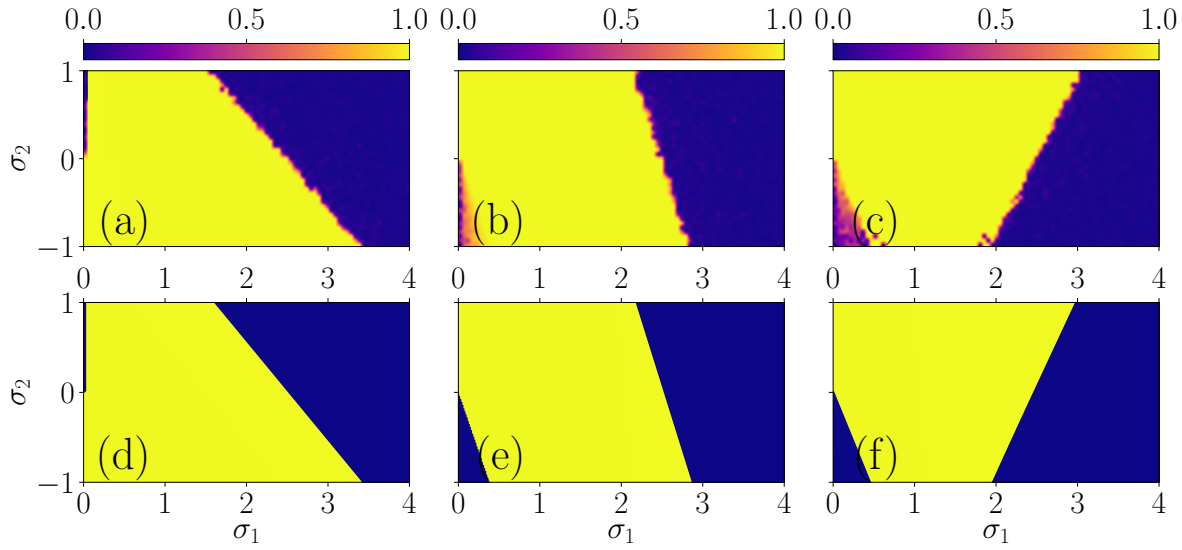

FIG. 5. Nonlocally connected Kuramoto oscillators with both pairwise and higher-order adaptations. Phase diagrams in the $\sigma_1 - \sigma_2$ plane depict the order parameter starting from a synchronization state with initial conditions close to $\theta_i(0) = 0$, $k_{ij}^{(1)} = -a_{ij}^{(1)} \sin\beta_1$ and $k_{ijp}^{(2)} = -a_{ijp}^{(2)} \sin\beta_2$, for three values of β_2: (a) $\beta_2 = 0.5\pi$, (b) $\beta_2 = 0.88\pi$, and (c) $\beta_2 = 1.2\pi$ for the case of adaptive higher-order Kuramoto model with lag. Panels (d)-(f) display the MSF for the adaptive Kuramoto model, wherein the regions with positive MLE are colored blue (dark), while those with negative MLE are yellow (bright). It is observed that the MSF is positive precisely where the order parameter R_c deviates from synchrony, i.e., $R_c = 1$ The remaining parameters were set fixed as in Fig. 4 and the number of connected oscillators on the both sides of the ring is $k = 30$.

However, for $\sigma_2 > 0$, we again observe a scenario opposite to the pairwise adaptation case, where decreasing σ_2 leads to a broader synchronization region. Finally, for $\beta_2 > \beta_1$ [Fig.5(c,e)], the system exhibits a similar trend to the case without higher-order adaptation: as σ_2 increases from negative to positive, the synchronization region widens. However, in the negative σ_2 regime, a prominent bounded region of synchrony is observed, resulting in a relatively narrower stable synchronization region compared to the pairwise adaptation scenario.

Thus, the results with nonlocal connection topology strengthen our finding that the introduction of higher-order adaptation leads to qualitatively different behaviors compared to the case without it, depending on the higher-order adaptive coupling.

B. Different ϵ_1 and ϵ_2

As previously mentioned, the preceding dimension reduction analysis with generic coupling functions is only feasible when $\epsilon_1 = \epsilon_2$. However, to what extent can it predict the stable synchronized region when $\epsilon_1 \neq \epsilon_2$? In this regard, here, we consider a scenario of unequal ϵ_1 and ϵ_2, and we thus challenge the theory presented so far under the assumption $\epsilon_1 = \epsilon_2$, to test its validity beyond the latter assumption. To do so we again consider the coupled Kuramoto dynamics given by Eq. (44) with all-to-all connection topology. In Fig. 6(a), we numerically calculate the order parameter for the case with $\epsilon_1 = 0.01$, $\epsilon_2 = 0.011$, and $\beta_1 = \beta_2 = 0.88\pi$. We observe that the analytical prediction with $\epsilon_1 = \epsilon_2 = 0.01$ [Fig. 4(e)] is capable of determining the synchronization reasonably well for this small parameter mismatch.

However, if we plug two different values of ϵ_1 and ϵ_2 (in place of $\epsilon_1 = \epsilon_2$) in the $\dot{\hat{\chi}}_i$ and $\dot{\hat{\eta}}_i$ equations of MSE (42) we can observe that the analytical prediction with this relatively small parameter mismatch [see Fig. 6(b)] is not capable of determining the synchronization reasonably well for a large set of parameters (σ_1, σ_2). Thus, the above observation reasserts the fact that the dimension reduction analysis for generic coupling function is valid only with $\epsilon_1 = \epsilon_2$.

IV. CONCLUSION

Summing up, we hereby provide a profound theoretical approach to study collective phenomena, specifically the synchronization, under the combined effect of higher-order interactions and adaptive connectivity. By assuming pairwise and higher-order structures to be regular or by considering noninvasive coupling functions, we have derived the necessary conditions for the stable synchronous solution to exist. Furthermore, we have shown that for two relevant settings, i.e., all-to-all and ring-like, the developed theory resembles the classical MSE approach and thus significantly reduces the intricacy of analytical calculations due to the presence of both adaptivity and higher-order interactions. Finally, our analyt-

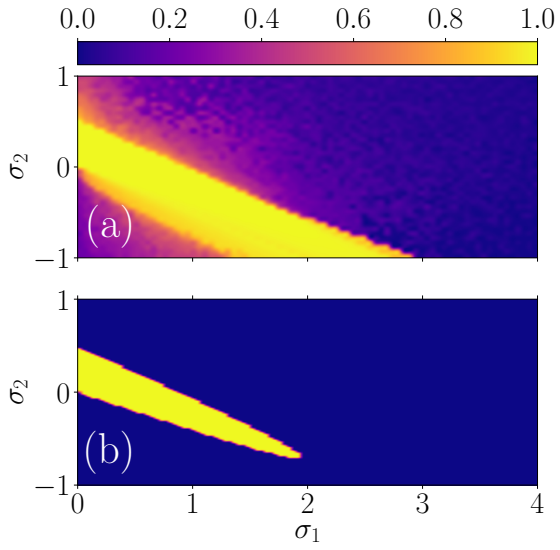

FIG. 6. Phase diagrams in the $\sigma_1 - \sigma_2$ plane showing (a) the order parameter, numerically computed for $\beta_2 = 0.88\pi$, and (b) the MSF obtained from analytical derivations, presented for the case of an adaptive higher-order Kuramoto model with lag, all-to-all coupling, and $\epsilon_1 \neq \epsilon_2$. Regions associated with positive Lyapunov exponents, indicating asynchronous regimes, are colored blue (dark), and the yellow (bright) regions correspond to negative MSF, hence to synchronization. Other parameters are fixed as in Fig. 4(b,e) with $\epsilon_1 = 0.01$ and $\epsilon_2 = 0.011$.

ical findings have been supported by dedicated numerical simulations, which have fully confirmed the validity of the approach. Additionally, our results highlight how our technique crucially incorporates the fundamental presence of higher-order interactions in adaptive networks, which previously could not be addressed. Our case studies show that the system displays markedly different behaviors when comparing scenarios with and without higher-order adaptation.

We note that the provided theoretical approach leads to a necessary condition that depends only on the interaction strengths and underlying structural properties of the higher-order structure. Thus, the fact that our approach can be used irrespective of any specific model or choice of coupling functions offers the possibility of extending it to different coupling mechanisms and systems, even those with single or distributed delays [70]. One of the most realistic examples of a complex system where both higher-order interactions and adaptivity play a pivotal role is the neuronal network. Our generalized approach, therefore, may provide a powerful tool for investigating collective phenomena in neuronal networks, even those involving synaptic plasticity [71]. Apart from the neuronal networks, adaptation is widely recognized in control theory [72, 73]. Our theoretical approach, therefore, offers a versatile framework for examining various adaptive control schemes across a broad spectrum of dynamical systems, including those with many-body interactions.

ACKNOWLEDGMENTS

The work of S.N.J. and P.M. is supported by MoE RUSA 2.0 (Bharathidasan University - Physical Sciences).

[1] A. Pikovsky, M. Rosenblum, and J. Kurths, *Synchronization: A Universal Concept in Nonlinear Sciences*, Cambridge Nonlinear Science Series (Cambridge University Press, 2001).
[2] A. Arenas, A. Díaz-Guilera, J. Kurths, Y. Moreno, and C. Zhou, Phys. Rep. **469**, 93 (2008).
[3] S. Boccaletti, A. N. Pisarchik, C. I. Del Genio, and A. Amann, *Synchronization: from coupled systems to complex networks* (Cambridge University Press, 2018).
[4] A.-L. Barabási, *Network science* (Cambridge University Press, 2016).
[5] D. S. Bassett, N. F. Wymbs, M. A. Porter, P. J. Mucha, J. M. Carlson, and S. T. Grafton, PNAS **108**, 7641 (2011).
[6] S. Wasserman and K. Faust, *Social Network Analysis: Methods and Applications* (Cambridge University Press, 1994).
[7] P. Holme and J. Saramäki, Phys. Rep. **519**, 97 (2012).
[8] A. H. Sayed, Proc. IEEE **102**, 460 (2014).
[9] T. Gross and H. Sayama, *Adaptive networks* (Springer, 2009).
[10] R. Berner, T. Gross, C. Kuehn, J. Kurths, and S. Yanchuk, Phys. Rep. **1031**, 1 (2023).
[11] J. Sawicki, R. Berner, S. A. M. Loos, M. Anvari, R. Bader, W. Barfuss, N. Botta, N. Brede, I. Franović, *et al.*, Chaos **33**, 071501 (2023).
[12] H. Markram, J. Lübke, M. Frotscher, and B. Sakmann, Science **275**, 213 (1997).
[13] L. F. Abbott and S. B. Nelson, Nat. Neurosci. **3**, 1178 (2000).
[14] C. Meisel and T. Gross, Phys. Rev. E **80**, 061917 (2009).
[15] L. Lücken, O. V. Popovych, P. A. Tass, and S. Yanchuk, Phys. Rev. E **93**, 032210 (2016).
[16] S. Jain and S. Krishna, PNAS **98**, 543 (2001).
[17] T. Gross, C. J. D. D'Lima, and B. Blasius, Phys. Rev. Lett. **96**, 208701 (2006).
[18] T. Gross and B. Blasius, J. R. Soc. Interface. **5**, 259 (2008).
[19] R. Berner, S. Vock, E. Schöll, and S. Yanchuk, Phys. Rev. Lett. **126**, 028301 (2021).
[20] R. Berner and S. Yanchuk, Front. Appl. Math. **7**, 714978 (2021).

[21] M. Thiele, R. Berner, P. A. Tass, E. Schöll, and S. Yanchuk, Chaos **33**, 023123 (2023).
[22] R. Berner, J. Sawicki, and E. Schöll, Phys. Rev. Lett. **124**, 088301 (2020).
[23] M. Manoranjani, V. R. Saiprasad, R. Gopal, D. V. Senthilkumar, and V. K. Chandrasekar, Phys. Rev. E **108**, 044307 (2023).
[24] M. Lodi, S. Panahi, F. Sorrentino, A. Torcini, and M. Storace, Commun. Phys. **7**, 198 (2024).
[25] R. Gutiérrez, A. Amann, S. Assenza, J. Gómez-Gardenes, V. Latora, and S. Boccaletti, Phys. Rev. Lett. **107**, 234103 (2011).
[26] X. Zhang, S. Boccaletti, S. Guan, and Z. Liu, Phys. Rev. Lett. **114**, 038701 (2015).
[27] D. Ghosh, M. Frasca, A. Rizzo, S. Majhi, S. Rakshit, K. Alfaro-Bittner, and S. Boccaletti, Phys. Rep. **949**, 1 (2022).
[28] V. Kohar, P. Ji, A. Choudhary, S. Sinha, and J. Kurths, Phys. Rev. E **90**, 022812 (2014).
[29] D. J. Stilwell, E. M. Bollt, and D. G. Roberson, SIAM J. Appl. Dyn. **5**, 140 (2006).
[30] T. Carletti and D. Fanelli, Chaos Soliton Fract. **159**, 112180 (2022).
[31] M. S. Anwar, S. Rakshit, D. Ghosh, and E. M. Bollt, Phys. Rev. E **105**, 024303 (2022).
[32] F. Battiston, G. Cencetti, I. Iacopini, V. Latora, M. Lucas, A. Patania, J.-G. Young, and G. Petri, Phys. Rep. **874**, 1 (2020).
[33] F. Battiston, E. Amico, A. Barrat, G. Bianconi, G. Ferraz de Arruda, B. Franceschiello, I. Iacopini, S. Kéfi, V. Latora, Y. Moreno, *et al.*, Nat. Phys. **17**, 1093 (2021).
[34] S. Boccaletti, P. De Lellis, C. I. del Genio, K. Alfaro-Bittner, R. Criado, S. Jalan, and M. Romance, Phys. Rep. **1018**, 1 (2023).
[35] S. Majhi, M. Perc, and D. Ghosh, J. R. Soc. Interface. **19**, 20220043 (2022).
[36] G. Bianconi, *Higher-order networks: An introduction to simplicial compelxes* (Cambridge University Press, 2021).
[37] C. Berge, *Graphs and hypergraphs*, North-Holland Pub. Co. (American Elsevier Pub. Co, 1973).
[38] I. Iacopini, G. Petri, A. Barrat, and V. Latora, Nat. Commun. **10**, 2485 (2019).
[39] T. Carletti, F. Battiston, G. Cencetti, and D. Fanelli, Phys. Rev. E **101**, 022308 (2020).
[40] M. T. Schaub, A. R. Benson, P. Horn, G. Lippner, and A. Jadbabaie, SIAM Rev. **62**, 353 (2020).
[41] L. Neuhäuser, R. Lambiotte, and M. T. Schaub, Phys. Rev. E **104**, 064305 (2021).
[42] R. Muolo, L. Gallo, V. Latora, M. Frasca, and T. Carletti, Chaos Soliton Fract. **166**, 112912 (2023).
[43] S. Gao, L. Chang, M. Perc, and Z. Wang, Phys. Rev. E **107**, 014216 (2023).
[44] T. Carletti, D. Fanelli, and S. Nicoletti, J. Phys.: Complex. **1**, 035006 (2020).
[45] P. S. Skardal and A. Arenas, Commun. Phys. **3**, 1 (2020).
[46] P. S. Skardal and A. Arenas, Phys. Rev. Lett. **122**, 248301 (2019).
[47] T. Carletti, L. Giambagli, and G. Bianconi, Phys. Rev. Lett. **130**, 187401 (2023).
[48] M. S. Anwar and D. Ghosh, Chaos **32**, 033125 (2022).
[49] M. S. Anwar and D. Ghosh, Phys. Rev. E **106**, 034314 (2022).
[50] S. N. Jenifer, D. Ghosh, and P. Muruganandam, Phys. Rev. E **109**, 054302 (2024).
[51] L. V. Gambuzza, F. Di Patti, L. Gallo, S. Lepri, M. Romance, R. Criado, M. Frasca, V. Latora, and S. Boccaletti, Nat. Commun. **12**, 1255 (2021).
[52] M. S. Anwar and D. Ghosh, SIAM J. Appl. Dyn. **22**, 2054 (2023).
[53] F. Parastesh, M. Mehrabbeik, K. Rajagopal, S. Jafari, and M. Perc, Chaos **32**, 013125 (2022).
[54] M. Mehrabbeik, S. Jafari, and M. Perc, Front. Comput. Neurosci **17**, 1248976 (2023).
[55] M. S. Anwar, G. K. Sar, M. Perc, and D. Ghosh, Commun. Phys. **7**, 59 (2024).
[56] R. Ghosh, U. K. Verma, S. Jalan, and M. D. Shrimali, Phys. Rev. E **108**, 044207 (2023).
[57] M. S. Anwar, N. Frolov, A. E. Hramov, and D. Ghosh, Phys. Rev. E **109**, 014225 (2024).
[58] A. Tlaie, I. Leyva, and I. Sendiña-Nadal, Phys. Rev. E **100**, 052305 (2019).
[59] S.-i. Amari, H. Nakahara, S. Wu, and Y. Sakai, Neural Comput. **15**, 127 (2003).
[60] A. D. Kachhvah and S. Jalan, Phys. Rev. E **105**, L062203 (2022).
[61] P. Rajwani, A. Suman, and S. Jalan, Chaos **33**, 061102 (2023).
[62] S. Dutta, P. Kundu, P. Khanra, C. Hens, and P. Pal, Transition to synchronization in adaptive sakaguchi-kuramoto model with higher-order interactions (2024), arXiv:2406.04701 [nlin.AO].
[63] A. A. Emelianova and V. I. Nekorkin, Chaos **34**, 023112 (2024).
[64] H. Fujisaka and T. Yamada, Prog. Theor. Phys. **69**, 32 (1983).
[65] L. M. Pecora and T. L. Carroll, Phys. Rev. Lett. **80**, 2109 (1998).
[66] M. S. Anwar, D. Ghosh, and T. Carletti, J. Phys.: Complex. **5**, 015020 (2024).
[67] R. Berner, E. Scholl, and S. Yanchuk, SIAM J. Appl. Dyn. **18**, 2227 (2019).
[68] D. V. Kasatkin, S. Yanchuk, E. Schöll, and V. I. Nekorkin, Phys. Rev. E **96**, 062211 (2017).
[69] D. V. Kasatkin and V. I. Nekorkin, Eur. Phys. J.: Spec. Top. **227**, 1051 (2018).
[70] Y. N. Kyrychko, K. B. Blyuss, and E. Schöll, Chaos **24**, 043117 (2014).
[71] O. V. Popovych, M. N. Xenakis, and P. A. Tass, PloS one **10**, e0117205 (2015).
[72] P. DeLellis, F. Garofalo, M. Porfiri, *et al.*, IEEE Trans. Circuits Syst. I: Regul. Pap. **57**, 2132 (2010).
[73] W. Yu, P. DeLellis, G. Chen, M. Di Bernardo, and J. Kurths, IEEE Trans. Autom. Control **57**, 2153 (2012).

Appendix A: non-invasive couplings

Here, we assume the pairwise and three-body coupling functions to be non-invasive, i.e., $g^{(1)}(s,s)=0$ and $g^{(2)}(s,s,s)=0$.

1. Only pairwise adaptation

In this case, the synchronized solution evolves according to the following equations,

$$\dot{\mathbf{s}} = f(\mathbf{s}), \tag{A1a}$$
$$k_{ij}^{(s)} = -a_{ij}^{(1)} h(0). \tag{A1b}$$

To analyze the stability of this synchronized state, we slightly perturb the system around the synchronized state with small perturbations $\xi_i = \mathbf{x}_i - \mathbf{s}$ and $\chi_{ij} = k_{ij}^{(1)} - k_{ij}^{(s)}$. Then, the variational equation can be written as

$$\begin{aligned}\dot{\xi}_i =& Df(\mathbf{s})\xi_i - \sigma_1 h(0) \sum_{j=1}^{N} L_{ij}^{(1)} D_2 g^{(1)}(\mathbf{s},\mathbf{s})\xi_j \\ &+ \sigma_2 \sum_{j=1}^{N} L_{ij}^{(2)} [D_2 g^{(2)}(\mathbf{s},\mathbf{s},\mathbf{s}) + D_3 g^{(2)}(\mathbf{s},\mathbf{s},\mathbf{s})]\xi_j,\end{aligned} \tag{A2a}$$

$$\dot{\chi}_{ij} = -\epsilon \left(\chi_{ij} + a_{ij}^{(1)} [Dh(0)(\xi_i - \xi_j)] \right). \tag{A2b}$$

In matrix form, the variational equation becomes

$$\begin{bmatrix} \dot{\boldsymbol{\xi}} \\ \dot{\boldsymbol{\chi}} \end{bmatrix} = \begin{bmatrix} \mathbf{S} & 0 \\ -\epsilon \mathbf{C}^{(1)} \otimes Dh(0) & -\epsilon \mathbf{I}_{N^2} \end{bmatrix} \begin{bmatrix} \boldsymbol{\xi} \\ \boldsymbol{\chi} \end{bmatrix}, \tag{A3}$$

where

$$\mathbf{S} = \mathbf{I}_N \otimes Df(s) - \sigma_1 h(0) \mathbf{L}^{(1)} \otimes D_2 g^{(1)} + \sigma_2 \mathbf{L}^{(2)} \otimes D_s g^{(2)},$$

with $D_s g^{(2)} = D_2 g^{(2)}(s,s,s) + D_3 g^{(2)}(s,s,s)$. $\mathbf{C}^{(1)}$ is a constant matrix of order $N^2 \times N$ (details are provided in the Appendix B).

To determine the stability condition for the associated synchronous solution, one needs to solve the system of equations (A3) to calculate the maximum Lyapunov exponents. The form of Eq. (A3) implies that the Jacobian matrix possesses N^2 numbers of $-\epsilon$ eigenvalues. Furthermore, it is a lower diagonal block matrix. Hence, the stability of $\mathbf{S}$, i.e., finding the maximum Lyapunov exponents by solving $\dot{\boldsymbol{\xi}} = \mathbf{S}\boldsymbol{\xi}$ provides the necessary condition for the stable synchronized solution, subject to $\epsilon > 0$. Now, $\dot{\boldsymbol{\xi}} = \mathbf{S}\boldsymbol{\xi}$ is a coupled linear differential equation of dimension Nd. To further simplify it, we project the projection variables ξ onto the eigenspace of the pairwise Laplacian matrix $\mathbf{L}^{(1)}$ by introducing a new set of variables $\boldsymbol{\zeta} = (\mathbf{U} \otimes \mathbf{I}_d)^\top \boldsymbol{\xi}$. Here, $\mathbf{U}$ is a $N \times N$ matrix whose columns are the orthonormal eigenvectors of the Laplacian $\mathbf{L}^{(1)}$, i.e., $\mathbf{U}^\top \mathbf{L}^{(1)} \mathbf{U} = \mathrm{diag}\{0 = \mu_1^{(1)}, \mu_2^{(1)}, \ldots, \mu_N^{(1)}\}$. Using this new coordinate system, the variational equation becomes

$$\dot{\zeta}_i = [Df(s) - \sigma_1 h(0) \mu_i^{(1)} D_2 g^{(1)}]\zeta_i + \sigma_2 \sum_{j=1}^{N} \tilde{L}_{ij}^2 D_s g^{(2)} \zeta_j, \tag{A4}$$

where we introduced $\tilde{L}^{(2)} = U^\top L^{(2)} U$ whose entries on the first row and column are all zero. Thus, ζ_1 corresponds to the modes parallel to the synchronous solution, and $\zeta_i,\ i = 2, 3, \ldots, N$ is associated with the transverse modes. In general, this transverse variation equation can not decouple further. However, when the higher-order Laplacian is a scalar multiple of the pairwise one and in the scenario of commutating Laplacian matrices, the variational equation can be fully decoupled into N numbers of d-dimensional equation.

2. Both pairwise and higher-order adaptation

In this case, the synchronized solution follows

$$\dot{\mathbf{s}} = f(\mathbf{s}), \tag{A5a}$$
$$k_{ij}^{(1),s} = -a_{ij}^{(1)} h^{(1)}(0), \tag{A5b}$$
$$k_{ijp}^{(2),s} = -a_{ijp}^{(2)} h^{(2)}(0). \tag{A5c}$$

The corresponding variation equation can be written as,

$$\begin{aligned}\dot{\xi}_i =& Df(\mathbf{s})\xi_i - \sigma_1 h^{(1)}(0) \sum_{j=1}^{N} L_{ij}^{(1)} D_2 g^{(1)}(\mathbf{s},\mathbf{s})\xi_j \\ &- \sigma_2 h^{(2)}(0) \sum_{j=1}^{N} L_{ij}^{(2)} (D_2 g^{(2)}(\mathbf{s},\mathbf{s},\mathbf{s}) + D_3 g^{(2)}(\mathbf{s},\mathbf{s},\mathbf{s}))\xi_j \\ &- \sigma_1 \sum_{j=1}^{N} a_{ij}^{(1)} \chi_{ij} g^{(1)}(\mathbf{s},\mathbf{s}) - \sigma_2 \sum_{j=1}^{N} \sum_{p=1}^{N} a_{ijp}^{(2)} \eta_{ijp} g^{(2)}(\mathbf{s},\mathbf{s},\mathbf{s}),\end{aligned} \tag{A6a}$$

$$\dot{\chi}_{ij} = -\epsilon_1 (\chi_{ij} + a_{ij}^{(1)} Dh^{(1)}(0)(\xi_i - \xi_j)), \tag{A6b}$$
$$\dot{\eta}_{ijp} = -\epsilon_2 (\eta_{ijp} + a_{ijp}^{(2)} Dh^{(2)}(0)(2\xi_i - \xi_j - \xi_p)). \tag{A6c}$$

Then, in matrix form, the variational equations can be written as

$$\begin{bmatrix} \dot{\boldsymbol{\xi}} \\ \dot{\boldsymbol{\chi}} \\ \dot{\eta} \end{bmatrix} = \begin{bmatrix} \mathbf{S}_2 & 0 & 0 \\ -\epsilon_1 \mathbf{C}^{(1)} \otimes Dh^{(1)}(0) & -\epsilon_1 \mathbf{I}_{N^2} & 0 \\ -\epsilon_2 \mathbf{C}^{(2)} \otimes Dh^{(2)}(0) & 0 & -\epsilon_2 \mathbf{I}_{N^3} \end{bmatrix} \begin{bmatrix} \boldsymbol{\xi} \\ \boldsymbol{\chi} \\ \boldsymbol{\eta} \end{bmatrix} \tag{A7}$$

where

$$\begin{aligned}\mathbf{S}_2 = \mathbf{I}_N \otimes Df(s) &- \sigma_1 h^{(1)}(0) \mathbf{L}^{(1)} \otimes D_2 g^{(1)} \\ &- \sigma_2 h^{(2)}(0) \mathbf{L}^{(2)} \otimes D_s g^{(2)}.\end{aligned}$$

To determine the stability condition for the associated synchronous solution, one needs to solve the above system of variation equations to calculate the maximum Lyapunov exponents. The form of the equation implies that the Jacobian matrix possesses N^2 numbers of $-\epsilon_1$ eigenvalues and N^3 numbers of ϵ_2 eigenvalues. Furthermore, it is a lower diagonal block matrix. Hence, the

stability of $\mathbf{S}_2$, i.e., finding the maximum Lyapunov exponents by solving $\dot{\boldsymbol{\xi}} = \mathbf{S}_2\,\boldsymbol{\xi}$ provides the necessary condition for the stable synchronized solution, subject to $\epsilon_1, \epsilon_2 > 0$. Further simplification of the variation equation $\dot{\boldsymbol{\xi}} = \mathbf{S}_2\,\boldsymbol{\xi}$ can be done similarly to the previous case. Hence, in this case, we can analytically predict the stability of the synchronous solution even if ϵ_1 and ϵ_2 are different.

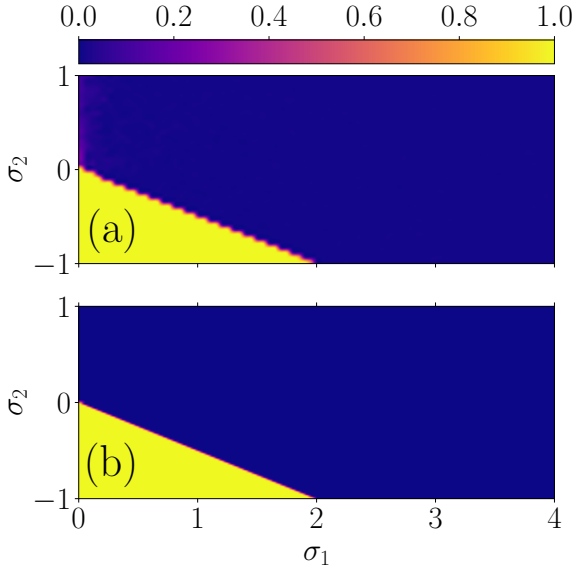

FIG. 7. Phase diagrams in the $\sigma_1 - \sigma_2$ plane showing (a) the order parameter, numerically computed for $\beta_2 = 0.88\pi$, and (b) the MSF obtained from analytical derivations, for the case of a higher-order Kuramoto model with lag, all-to-all topology having both pairwise and higher-order adaptation, and noninvasive coupling schemes. Regions associated with positive Lyapunov exponents, indicating asynchronous regimes, are colored blue (dark), whereas yellow (bright) represents the region of negative Lyapunov exponents. Other parameters are fixed as follows: $N = 100$, $\alpha_1 = \alpha_2 = 0$, $\beta_1 = \beta_2 = 0.88\pi$, $\epsilon_1 = 0.01$, $\epsilon_2 = 0.02$.

To show that the presented theory corresponding to the noninvasive coupling works even for $\epsilon_1 \neq \epsilon_2$, we consider an ensemble of $N = 100$ globally coupled phase-lagged Kuramoto oscillators given by Eq. (44). Since the coupling functions $g^{(i)}$, $i = 1, 2$ are synchronization noninvasive, we consider the lag parameters $\alpha_i = 0$. The time scale separation parameters are taken as $\epsilon_1 = 0.01$ and $\epsilon_2 = 0.02$. All the other parameters are kept fixed at a nominal value. The results are reported in Fig. 7 where the MSF [see Fig. 7(b)] is computed as a function of σ_1 and σ_2 and compared with the order parameter R_c [see Fig. 7(a)]. It is observable that the analytical prediction can determine the region of stable synchronous solution very well.

Appendix B: Derivation of the master stability equations

Here, we provide a detailed, step-by-step derivation of the master stability equations discussed in the main text.

1. Derivation of the master stability equation for the system with pairwise adaptation and constant higher-order interactions

The general dynamical equations of the adaptive higher-order networks with adaptation only in pairwise interactions are given by

$$\dot{\mathbf{x}}_i = f(\mathbf{x}_i) - \sigma_1 \sum_{j=1}^{N} a_{ij}^{(1)} k_{ij}^{(1)}(t) g^{(1)}(\mathbf{x}_i, \mathbf{x}_j) - \sigma_2 \sum_{j=1}^{N}\sum_{p=1}^{N} a_{ijp}^{(2)} k_{ijp}^{(2)} g^{(2)}(\mathbf{x}_i, \mathbf{x}_j, \mathbf{x}_p), \tag{B1a}$$

$$\dot{k}_{ij}^{(1)} = -\epsilon[k_{ij}^{(1)} + a_{ij}^{(1)} h(\mathbf{x}_i - \mathbf{x}_j)], \tag{B1b}$$

where the adjacency matrix (tensor) satisfies the constant degree property for each node, i.e., $\sum a_{ij}^{(1)} = r^{(1)}$ and $\sum_{j=1}^{N}\sum_{p=1}^{N} a_{ijp}^{(2)} = 2r^{(2)}$. Let us observe that $(\mathbf{s}, k^{(s)})$ is the synchronized solution for the adaptive dynamical system when it satisfies the following evolution equations:

$$\dot{\mathbf{s}} = f(\mathbf{s}) + \sigma_1 r^{(1)} h(0) g^{(1)}(\mathbf{s}, \mathbf{s}) - 2\sigma_2 r^{(2)} g^{(2)}(\mathbf{s}, \mathbf{s}, \mathbf{s}), \tag{B2a}$$

$$k_{ij}^{(s)} = -a_{ij}^{(1)} h(0). \tag{B2b}$$

Now, to analyze the stability of this synchronized state, we slightly perturb the system around the synchronized state with the perturbations defined as $\xi_i = \mathbf{x}_i - \mathbf{s}$ and $\chi_{ij} = k_{ij}^{(1)} - k_{ij}^{(s)}$. Using Taylor series expansion to linearize the system around the synchronized state, we can obtain the variational equations as follows,

$$\dot{\xi}_i = Df(\mathbf{s})\xi_i - \sigma_1 \sum_{j=1}^{N} a_{ij}^{(1)} g^{(1)}(\mathbf{s}, \mathbf{s})\chi_{ij} + \sigma_1 r^{(1)} h(0) D_1 g^{(1)}(\mathbf{s}, \mathbf{s})\xi_i + \sigma_1 h(0) \sum_{j=1}^{N} a_{ij}^{(1)} D_2 g^{(1)}(\mathbf{s}, \mathbf{s})\xi_j - 2\sigma_2 r^{(2)} D_1 g^{(2)}(\mathbf{s}, \mathbf{s}, \mathbf{s})\xi_i - \sigma_2 \sum_{j=1}^{N}\sum_{p=1}^{N} a_{ijp}^{(2)} [D_2 g^{(2)}(\mathbf{s}, \mathbf{s}, \mathbf{s})\xi_j + D_3 g^{(2)}(\mathbf{s}, \mathbf{s}, \mathbf{s})\xi_p], \tag{B3a}$$

$$\dot{\chi}_{ij} = -\epsilon(\chi_{ij} + a_{ij}^{(1)}[Dh(0)(\xi_j - \xi_i)], \tag{B3b}$$

where Df and $Dh^{(1)}$ are the Jacobians of f and h, $D_i g^{(j)}$ denotes the Jacobian of the function g^j, $(j = 1, 2)$, with respect to the i-th variables, $i = 1, 2, 3$.

By introducing the pairwise and higher-order Laplacians $\mathbf{L}^{(1)}$ and $\mathbf{L}^{(2)}$, defined as

$$L_{ij}^{(1)} = \begin{cases} -a_{ij}^{(1)}, & i \neq j \\ \sum\limits_{j=1}^{N} a_{ij}^{(1)} = r^{(1)}, & i = j \end{cases} \tag{B4}$$

and,

$$L_{ij}^{(2)} = \begin{cases} -\sum\limits_{k=1}^{N} a_{ijk}^{(2)}, & i \neq j \\ \sum\limits_{j=1}^{N}\sum\limits_{k=1}^{N} a_{ijk}^{(2)} = 2r^{(2)}, & i = j \end{cases} \tag{B5}$$

we can rewrite the variational equation as,

$$\begin{aligned} \dot{\xi}_i =& Df(\mathbf{s})\xi_i - \sigma_1 \sum_{j=1}^{N} a_{ij}^{(1)} g^{(1)}(\mathbf{s},\mathbf{s})\chi_{ij} + \sigma_1 r^{(1)} h(0)[D_1 g^{(1)}(\mathbf{s},\mathbf{s}) + D_2 g^{(1)}(\mathbf{s},\mathbf{s})]\xi_i \\ & - \sigma_1 h(0) \sum_{j=1}^{N} L_{ij}^{(1)} D_2 g^{(1)}(\mathbf{s},\mathbf{s})\xi_j - 2\sigma_2 r^{(2)}[D_1 g^{(2)}(\mathbf{s},\mathbf{s},\mathbf{s}) + D_2 g^{(2)}(\mathbf{s},\mathbf{s},\mathbf{s}) + D_3 g^{(2)}(\mathbf{s},\mathbf{s},\mathbf{s})]\xi_i \\ & + \sigma_2 \sum_{j=1}^{N} L_{ij}^{(2)}[D_1 g^{(2)}(\mathbf{s},\mathbf{s},\mathbf{s}) + D_2 g^{(2)}(\mathbf{s},\mathbf{s},\mathbf{s})]\xi_j \end{aligned} \tag{B6}$$

and

$$\dot{\chi}_{ij} = -\epsilon(\kappa_{ij} + a_{ij}[Dh(0)(\xi_j - \xi_i)]. \tag{B7}$$

Now, to write the variational equation in matrix form, we introduce the vectorized form for the perturbations as $\xi = \mathbf{x} - I_N \otimes \mathbf{s}$ and $\chi = k - k^s$ with

$$\begin{aligned} \mathbf{x} =& (\mathbf{x}_1^\top, \ldots, \mathbf{x}_N^\top)^\top, \\ k =& (k_{11}, \ldots, k_{1N}, k_{21}, \ldots, k_{2N}, \ldots, k_{N1}, \ldots, k_{NN})^\top, \end{aligned} \tag{B8}$$

where we stack the rows of k_{ij} successively to make the $N \times N$ matrix χ_{ij} to a N^2 dimensional vector.

Thereafter, to proceed further we introduce few notations and matrices as follows. We consider

$$\mathbf{a}_i^{(1)} = (a_{i1}^{(1)}, \ldots, a_{iN}^{(1)}), \quad \mathrm{diag}(\mathbf{a}_i^{(1)}) = \begin{pmatrix} a_{i1}^{(1)} & & \\ & \cdots & \\ & & a_{iN}^{(1)} \end{pmatrix}$$

and the $N \times N^2$, $N^2 \times N$ matrices as,

$$\mathbf{B}^{(1)} = \begin{pmatrix} \mathbf{a}_1^{(1)} & & \\ & \cdots & \\ & & \mathbf{a}_N^{(1)} \end{pmatrix}, \quad \mathbf{D}^{(1)} = \begin{pmatrix} \mathrm{diag}(\mathbf{a}_1^{(1)}) \\ \vdots \\ \mathrm{diag}(\mathbf{a}_N^{(1)}) \end{pmatrix}.$$

We further can construct the $\mathbf{C}^{(1)}$ matrix of dimension $N^2 \times N$ from $\mathbf{B}^{(1)}$ and $\mathbf{D}^{(1)}$ as,

$$\mathbf{C}^{(1)} = B^{(1)^\top} - \mathbf{D}^{(1)} \tag{B9}$$

Using all the above notations and matrices, the variational equation can be written in block matrix form as,

$$\begin{pmatrix} \dot{\boldsymbol{\xi}} \\ \dot{\boldsymbol{\chi}} \end{pmatrix} = \begin{pmatrix} \mathbf{S} & -\sigma_1 \mathbf{B}^{(1)} \otimes g^{(1)}(\mathbf{s},\mathbf{s}) \\ -\epsilon \mathbf{C}^{(1)} \otimes Dh(0) & -\epsilon \mathbf{I}_{N^2} \end{pmatrix} \begin{pmatrix} \boldsymbol{\xi} \\ \boldsymbol{\chi} \end{pmatrix}, \tag{B10}$$

where $\mathbf{S} = \mathbf{I}_N \otimes Df(s) + \sigma_1 h(0)[r\mathbf{I}_N \otimes (D_1 g^{(1)} + D_2 g^{(1)})] - 2\sigma_2[r^{(2)}\mathbf{I}_N \otimes [D_1 g^{(2)} + D_2 g^{(2)} + D_3 g^{(2)}] - \sigma_1 h(0)\mathbf{L}^{(1)} \otimes D_2 g^{(1)} + \sigma_2 \mathbf{L}^{(2)} \otimes [D_2 g^{(2)} + D_3 g^{(2)}]$. $\mathbf{I}_N$ is the $N \times N$ identity matrix, $\mathbf{B}^{(1)}$ and $\mathbf{C}^{(1)}$ satisfy the relation $\mathbf{B}^{(1)}\mathbf{B}^{(1)^\top} = r^{(1)}\mathbf{I}_N$ and $\mathbf{B}^{(1)}\mathbf{C}^{(1)} = \mathbf{L}^{(1)}$.

From the structure of the variational equation, one can easily find that it has $(N^2 - N)$ eigenvalues $\lambda = -\epsilon$. The eigenspace corresponding to those eigenvalues are time-independent and can be obtained from,

$$\begin{pmatrix} \mathbf{S} + \epsilon \mathbf{I}_{Nd} & -\sigma_1 \mathbf{B}^{(1)} \otimes g^{(1)}(\mathbf{s},\mathbf{s}) \\ -\epsilon \mathbf{C}^{(1)} \otimes Dh(0) & 0 \end{pmatrix} \begin{pmatrix} \boldsymbol{\xi} \\ \boldsymbol{\chi} \end{pmatrix} = 0. \tag{B11}$$

From this it is obvious that $(\boldsymbol{\xi}, \boldsymbol{\chi})$ satisfying $\boldsymbol{\xi} = 0$ and $\mathbf{B}^{(1)}\boldsymbol{\chi} = 0$ are the time-independent eigenvectors. Now, since $\boldsymbol{\chi}$ is N^2 dimensional and $\mathrm{rank}(\mathbf{B}^{(1)}) = N$ when the row sum $r^{(1)}$ is nonzero, we can say that there exists $(N^2 - N)$ linearly independent eigenvectors which spans the eigenspace corresponding to the eigenvalue $-\epsilon$.

For the $(N^2 - N)$ eigenvalues, there exists $(N^2 - N)$ independent eigenvectors $v_l (l = 1, 2, \ldots, N^2 - N)$ spanning the kernal of $\mathbf{B}^{(1)}$. By using the Gram-Schmidt procedure, we can find the orthonormal basis for the kernel of

$\mathbf{B}^{(1)}$ as $\ker(\mathbf{B}^{(1)}) = \text{span}(y_1, \ldots, y_{N^2-N})$. With this basis, we can define matrices $\mathbf{R}^{(1)}$ and $\mathbf{Q}^{(1)}$ of dimensions $N^2 \times (N^2 - N)$ and $(N^2 + Nd) \times (N^2 + Nd)$, respectively as $\mathbf{R}^{(1)} = (y_1, y_2, \ldots, y_{N^2-N})$ and $\mathbf{Q}^{(1)}$,

$$\mathbf{Q}^{(1)} = \begin{pmatrix} \mathbf{I}_{Nd} & 0 & 0 \\ 0 & (1/r^{(1)})\mathbf{B}^{(1)^\top} & \mathbf{R}^{(1)} \end{pmatrix}. \tag{B12}$$

The left inverse of $\mathbf{Q}^{(1)}$ is

$$\mathbf{Q}^{(1)^{-1}} = \begin{pmatrix} \mathbf{I}_{Nd} & 0 \\ 0 & \mathbf{B}^{(1)} \\ 0 & \mathbf{R}^{(1)} \end{pmatrix}, \tag{B13}$$

So that, $\mathbf{Q}^{(1)^{-1}}\mathbf{Q}^{(1)} = \mathbf{I}_{N^2+Nd}$. The variational equation can be written as,

$$\begin{pmatrix} \dot{\boldsymbol{\xi}} \\ \dot{\boldsymbol{\chi}} \end{pmatrix} = \mathbf{Q}^{(1)^{-1}} \begin{pmatrix} \mathbf{S} & -\sigma_1 \mathbf{B}^{(1)} \otimes g^{(1)}(\mathbf{s}, \mathbf{s}) \\ -\epsilon \mathbf{C}^{(1)} \otimes Dh(0) & -\epsilon \mathbf{I}_{N^2} \end{pmatrix} \mathbf{Q}^{(1)} \begin{pmatrix} \boldsymbol{\xi} \\ \boldsymbol{\chi} \end{pmatrix}, \tag{B14}$$

where with a slight abuse we use the same letter to indicate the new transformed co-ordinates. Now,

$$\begin{aligned} \mathbf{Q}^{(1)^{-1}} \begin{pmatrix} \mathbf{S} & -\sigma_1 \mathbf{B}^{(1)} \otimes g^{(1)}(\mathbf{s}, \mathbf{s}) \\ -\epsilon \mathbf{C}^{(1)} \otimes Dh(0) & -\epsilon \mathbf{I}_{N^2} \end{pmatrix} \mathbf{Q}^{(1)} &= \mathbf{Q}^{(1)^{-1}} \begin{pmatrix} \mathbf{S} & -\sigma_1 \mathbf{B}^{(1)} \otimes g^{(1)}(\mathbf{s}, \mathbf{s}) \\ -\epsilon \mathbf{C}^{(1)} \otimes Dh(0) & -\epsilon \mathbf{I}_{N^2} \end{pmatrix} \\ &\quad \times \begin{pmatrix} \mathbf{I}_{Nd} & 0 & 0 \\ 0 & (1/r^{(1)})\mathbf{B}^{(1)^\top} & \mathbf{R}^{(1)} \end{pmatrix} \\ &= \mathbf{Q}^{(1)^{-1}} \begin{pmatrix} \mathbf{S} & -\sigma_1 \mathbf{I}_N \otimes g^{(1)}(\mathbf{s}, \mathbf{s}) & 0 \\ -\epsilon \mathbf{C}^{(1)} \otimes Dh(0) & -\epsilon / r^{(1)} \mathbf{B}^{(1)^\top} & -\epsilon \mathbf{R}^{(1)} \end{pmatrix} \\ &= \begin{pmatrix} \mathbf{I}_{Nd} & 0 \\ 0 & \mathbf{B}^{(1)} \\ 0 & \mathbf{R}^{(1)} \end{pmatrix} \begin{pmatrix} \mathbf{S} & -\sigma_1 \mathbf{I}_N \otimes g^{(1)}(\mathbf{s}, \mathbf{s}) & 0 \\ -\epsilon \mathbf{C}^{(1)} \otimes Dh(0) & -\epsilon / r^{(1)} \mathbf{B}^{(1)^\top} & -\epsilon \mathbf{R}^{(1)} \end{pmatrix} \\ &= \begin{pmatrix} \mathbf{S} & -\sigma_1 \mathbf{I}_N \otimes g^{(1)}(\mathbf{s}, \mathbf{s}) & 0 \\ -\epsilon \mathbf{L}^{(1)} \otimes Dh(0) & -\epsilon \mathbf{I}_N & 0 \\ -\epsilon \mathbf{R}^{(1)^\top} \mathbf{C}^{(1)} \otimes Dh(0) & 0 & -\epsilon \mathbf{I}_{N^2-N} \end{pmatrix} \end{aligned}$$

From this, we can obtain $(N + Nd)$ coupled master equations as

$$\begin{pmatrix} \dot{\boldsymbol{\xi}} \\ \dot{\boldsymbol{\chi}}_M \end{pmatrix} = \begin{pmatrix} \mathbf{S} & -\sigma_1 \mathbf{I}_N \otimes g^{(1)}(\mathbf{s}, \mathbf{s}) \\ -\epsilon \mathbf{L}^{(1)} \otimes Dh(0) & -\epsilon \mathbf{I}_N \end{pmatrix} \begin{pmatrix} \boldsymbol{\xi} \\ \boldsymbol{\chi}_M \end{pmatrix}, \tag{B15}$$

where $\boldsymbol{\chi}_M = \boldsymbol{\chi}_1$. Moreover, we yield $N^2 - N$ salve equations which can be solved explicitly once the variables associated with the master equations are known. This equations are given by

$$\dot{\boldsymbol{\chi}}_S = \begin{pmatrix} -\epsilon \mathbf{R}^{(1)^\top} \mathbf{C}^{(1)} \otimes Dh(0) & 0 & -\epsilon \mathbf{I}_{N^2-N} \end{pmatrix} \begin{pmatrix} \boldsymbol{\xi} \\ \boldsymbol{\chi}_M \\ \boldsymbol{\chi}_S \end{pmatrix}, \tag{B16}$$

where $\boldsymbol{\chi}_S = (\chi_2^\top, \chi_3^\top, \ldots, \chi_N^\top)^\top$. Now, corresponding to the zero row-sum symmetric Laplacian matrices there exists the matrices with its columns as orthonormal eigenvectors that diagonalize the Laplacian matrices. For example, there exists the matrix $\mathbf{U}$ such that $\mathbf{U}^\top \mathbf{L}^{(1)} \mathbf{U} = \mathbf{D}$, where $\mathbf{D}$ is the diagonal matrix with the diagonal entries being the eigenvalues of $\mathbf{L}^{(1)}$. In order to use this relation to decouple the master variational equation, we introduce a change of co-ordinates defined as

$$\begin{pmatrix} \mathbf{U} \otimes \mathbf{I}_d & 0 \\ 0 & \mathbf{U} \end{pmatrix} \begin{pmatrix} \boldsymbol{\xi} \\ \boldsymbol{\chi}_M \end{pmatrix} = \begin{pmatrix} \boldsymbol{\zeta} \\ \boldsymbol{\eta} \end{pmatrix}. \tag{B17}$$

This yields

$$\begin{pmatrix} \dot{\boldsymbol{\zeta}} \\ \dot{\boldsymbol{\eta}} \end{pmatrix} = \begin{pmatrix} \tilde{\mathbf{S}} & -\sigma_1 \mathbf{I}_N \otimes g^{(1)}(\mathbf{s}, \mathbf{s}) \\ -\epsilon \mathbf{D}_L^{(1)} \otimes Dh(0) & -\epsilon \mathbf{I}_N \end{pmatrix} \begin{pmatrix} \boldsymbol{\zeta} \\ \boldsymbol{\eta} \end{pmatrix}, \tag{B18}$$

where $\tilde{\mathbf{S}} = \mathbf{U}^\top \mathbf{S} \mathbf{U} = \mathbf{I}_N \otimes Df(s) + \sigma_1 h(0)[r^{(1)} \mathbf{I}_N \otimes (D_1 g^{(1)} + D_2 g^{(1)})] - 2\sigma_2 [r^{(2)} \mathbf{I}_N \otimes [D_1 g^{(2)} + D_2 g^{(2)} + D_3 g^{(2)}] - \sigma_1 h(0) \mathbf{D} \otimes D_2 g^{(1)} + \sigma_2 \mathbf{U}^H \mathbf{L}^{(2)} \mathbf{U} \otimes [D_2 g^{(2)} +$

$D_3 g^{(2)}]$. In explicit form it can be expressed as,

$$\dot{\zeta}_i = [Df(s) + \sigma_1 h(0) r^{(1)} Dg^{(1)} - \sigma_1 h(0) \mu_i^{(1)} D_2 g^{(1)} - 2\sigma_2 r^{(2)} Dg^{(2)}]\zeta_i + \sum_{j=1}^{N} \tilde{L}_{ij}^2 D_s \mathbf{g}^{(2)} \zeta_j - \sigma_1 g^{(1)}(s,s)\eta_i, \tag{B19a}$$

$$\dot{\eta}_i = -\epsilon[\mu_i^{(1)} Dh(0)\zeta_i + \eta_i], \tag{B19b}$$

with $\tilde{\mathbf{L}}^{(2)} = \mathbf{U}^\top \mathbf{L}^{(2)} \mathbf{U}$. This is the required master stability equation.

2. Derivation of the master stability equation for the system with both pairwise and higher-order adaptations

The general dynamical equations of the adaptive weighted simplicial complexes with adaptation in both pairwise and higher-order interactions are

$$\dot{\mathbf{x}}_i = f(\mathbf{x}_i) - \sigma_1 \sum_{j=1}^{N} a_{ij}^{(1)} k_{ij}^{(1)}(t) g^{(1)}(\mathbf{x}_i, \mathbf{x}_j) - \sigma_2 \sum_{j=1}^{N}\sum_{p=1}^{N} a_{ijp}^{(2)} k_{ijp}^{(2)}(t) g^{(2)}(\mathbf{x}_i, \mathbf{x}_j, \mathbf{x}_p), \tag{B20a}$$

$$\dot{k}_{ij}^{(1)} = -\epsilon_1[k_{ij}^{(1)} + a_{ij}^{(1)} h^{(1)}(\mathbf{x}_i - \mathbf{x}_j)], \tag{B20b}$$

$$\dot{k}_{ijp}^{(2)} = -\epsilon_2[k_{ijp}^{(2)} + a_{ijp}^{(2)} h^{(2)}(2\mathbf{x}_i - \mathbf{x}_j - \mathbf{x}_p)]. \tag{B20c}$$

The corresponding synchronized solution is given by,

$$\dot{\mathbf{s}} = f(\mathbf{s}) + \sigma_1 r^{(1)} h^{(1)}(0) g^{(1)}(\mathbf{s},\mathbf{s}) + 2\sigma_2 r^{(2)} h^{(2)}(0) g^{(2)}(\mathbf{s},\mathbf{s},\mathbf{s}), \tag{B21a}$$

$$k_{ij}^{(s)} = -a_{ij}^{(1)} h^{(1)}(0), \tag{B21b}$$

$$k_{ijp}^{(s)} = -a_{ijp}^{(2)} h^{(2)}(0). \tag{B21c}$$

A linear stability analysis about this solution can be performed to infer the existence of a synchronous solution. We thus perturb the system with small perturbation terms $\xi_i = \mathbf{x}_i - \mathbf{s}$, $\chi_{ij} = k_{ij}^{(1)} - k_{ij}^{(s)}$ and $\eta_{ijp} = k_{ijp}^{(2)} - k_{ijp}^{(s)}$, ans we study their time evolution via the variational equations

$$\dot{\xi}_i = Df(\mathbf{s})\xi_i + \sigma_1 r^{(1)} h^{(1)}(0) Dg^{(1)}(\mathbf{s},\mathbf{s})\xi_i + 2\sigma_2 r^{(2)} h^{(2)}(0) Dg^{(2)}(\mathbf{s},\mathbf{s},\mathbf{s})\xi_i - \sigma_1 h^{(1)}(0) \sum_{j=1}^{N} L_{ij}^{(1)} D_2 g^{(1)}(\mathbf{s},\mathbf{s})\xi_j + - \sigma_2 h^{(2)}(0) \sum_{j=1}^{N} L_{ij}^{(2)} D_s g^{(2)}(\mathbf{s},\mathbf{s},\mathbf{s})\xi_j - \sigma_1 \sum_{j=1}^{N} a_{ij}^{(1)} \chi_{ij} g^{(1)}(\mathbf{s},\mathbf{s}) - \sigma_2 \sum_{j=1}^{N}\sum_{p=1}^{N} a_{ijp}^{(2)} \eta_{ijp} g^{(2)}(\mathbf{s},\mathbf{s},\mathbf{s}), \tag{B22a}$$

$$\dot{\chi}_{ij} = -\epsilon_1(\chi_{ij} + a_{ij}^{(1)} Dh^{(1)}(0)(\xi_i - \xi_j)), \tag{B22b}$$

$$\dot{\eta}_{ijp} = -\epsilon_2(\eta_{ijp} + a_{ijp}^{(2)} Dh^{(2)}(0)(2\xi_i - \xi_j - \xi_p)), \tag{B22c}$$

where $Dg^{(1)} = D_1 g^{(1)} + D_2 g^{(1)}$, $Dg^{(2)} = D_1 g^{(2)} + D_2 g^{(2)} + D_3 g^{(2)}$ and $D_s g^{(2)} = D_2 g^{(2)} + D_3 g^{(2)}$.

Now, we consider $\xi = \mathbf{x} - I_N \otimes \mathbf{s}$, $\chi = k^{(1)} - k^s$ and $\eta = k^{(2)} - k^s$ with

$$\mathbf{x} = (\mathbf{x}_1^\top, \ldots, \mathbf{x}_N^\top)^\top,$$
$$k^{(1)} = (k_{11}^{(1)}, \ldots, k_{1N}^{(1)}, k_{21}^{(1)}, \ldots, k_{2N}^{(1)}, \ldots, k_{N1}^{(1)}, \ldots, k_{NN}^{(1)})^\top,$$
$$k^{(2)} = (k_{111}^{(2)}, \ldots, k_{1NN}^{(1)}, k_{211}^{(1)}, \ldots, k_{2NN}^{(1)}, \ldots, k_{N11}^{(1)}, \ldots, k_{NNN}^{(1)})^\top. \tag{B23}$$

Now analogous to the previous case here we again introduce few other notations and matrices to be used in the following derivations. We consider

$$\mathbf{a}_i^{(2)} = (a_{i11}^{(2)}, a_{i12}^{(2)}, \ldots, a_{iNN}^{(2)}),$$

and $N \times N^3$, $N^3 \times N$ matrices as,

$$\mathbf{B}^{(2)} = \begin{pmatrix} \mathbf{a}_1^{(2)} & & & \\ & \mathbf{a}_2^{(2)} & & \\ & & \cdots & \\ & & & \mathbf{a}_N^{(2)} \end{pmatrix},$$
$$\mathbf{C}^{(2)} = 2\mathbf{B}^{(2)^\top} - \mathbf{D}_1^{(2)} - \mathbf{D}_2^{(2)}, \tag{B24}$$

where the $N^3 \times N$ matrices $\mathbf{D}_1^{(2)}$ and $\mathbf{D}_2^{(2)}$ is given by

$$\mathbf{D}_1^{(2)} = \begin{pmatrix} d_1 \\ \vdots \\ d_N \end{pmatrix}, \quad \mathbf{D}_2^{(2)} = \begin{pmatrix} e_1 \\ \vdots \\ e_N \end{pmatrix}.$$

The elements of the matrices $\mathbf{D}_1^{(2)}$ and $\mathbf{D}_2^{(2)}$ are given for

$i = 1, 2, \ldots, N$ as

$$d_i = \begin{pmatrix} p_{i1} & & & \\ & p_{i2} & & \\ & & \cdots & \\ & & & p_{iN} \end{pmatrix}, \text{ and } e_i = \begin{pmatrix} q_{i1} \\ q_{i2} \\ \vdots \\ q_{iN} \end{pmatrix}$$

with

$$p_{ij} = \begin{pmatrix} a^{(2)}_{ij1} \\ a^{(2)}_{ij2} \\ \vdots \\ a^{(2)}_{ijN} \end{pmatrix}, \text{ and } q_{ij} = \begin{pmatrix} a^{(2)}_{ij1} & & & \\ & a^{(2)}_{ij2} & & \\ & & \cdots & \\ & & & a^{(2)}_{ijN} \end{pmatrix},$$

where $j = 1, 2, \ldots, N$. Using all these notations together, the variational equation in the block matrix form can be expressed as

$$\begin{bmatrix} \dot{\boldsymbol{\xi}} \\ \dot{\boldsymbol{\chi}} \\ \dot{\boldsymbol{\eta}} \end{bmatrix} = \begin{bmatrix} \mathbf{S}_2 & -\sigma_1 \mathbf{B}^{(1)} \otimes g^{(1)}(\mathbf{s}, \mathbf{s}) & -\sigma_2 \mathbf{B}^{(2)} \otimes g^{(2)}(\mathbf{s}, \mathbf{s}, \mathbf{s}) \\ -\epsilon_1 \mathbf{C}^{(1)} \otimes Dh^{(1)}(0) & -\epsilon_1 \mathbf{I}_{N^2} & 0 \\ -\epsilon_2 \mathbf{C}^{(2)} \otimes Dh^{(2)}(0) & 0 & -\epsilon_2 \mathbf{I}_{N^3} \end{bmatrix} \begin{bmatrix} \boldsymbol{\xi} \\ \boldsymbol{\chi} \\ \boldsymbol{\eta} \end{bmatrix}, \tag{B25}$$

where we consider again the matrix $\boldsymbol{\chi}$, resp. the tensor $\boldsymbol{\eta}$, as N^2, resp. N^3, columns vectors, and we introduce suitable matrix

$$\begin{aligned} \mathbf{S}_2 =& \mathbf{I}_N \otimes Df(fs) + \sigma_1 h^{(1)}(0)(r^{(1)} \mathbf{I}_N \otimes Dg^{(1)}) \\ &+ 2\sigma_2 h^{(1)}(0)(r^{(2)} \mathbf{I}_N \otimes Dg^{(2)}) - \sigma_1 h^{(1)}(0) \mathbf{L}^{(1)} \otimes D_2 g^{(1)} \\ &- \sigma_2 h^{(2)}(0) \mathbf{L}^{(2)} \otimes D_s g^{(2)}. \end{aligned} \tag{B26}$$

$\mathbf{B}^{(1)}$ and $\mathbf{C}^{(1)}$ are the same constant matrices of order $N \times N^2$ and $N^2 \times N$ used in Section B 1, while $\mathbf{B}^{(2)}$ and $\mathbf{C}^{(2)}$ are constant matrices of order $N \times N^3$ and $N^3 \times N$, satisfying $\mathbf{B}^{(2)} \mathbf{B}^{(2)^\top} = 2r^{(2)} \mathbf{I}_N$ and $\mathbf{B}^{(2)} \mathbf{C}^{(2)} = \mathbf{L}^{(2)}$.

Now to move forward we consider $\epsilon_1 = \epsilon_2 = \epsilon$. Then, from the structure of the variational equation, it is obvious that it has $(N^3 + N^2 - 2N)$ numbers of eigenvalues $\lambda = -\epsilon$. Thereafter proceeding similarly as the pairwise adaptation case, we can define two matrices $\mathbf{Q}^{(2)}$ and $\mathbf{R}^{(2)}$ as,

$$\mathbf{Q}^{(2)} = \begin{pmatrix} \mathbf{I}_{Nd} & 0 & 0 & 0 \\ 0 & (1/r^{(1)}) \mathbf{B}^{(1)^\top} & 0 & 0 \\ 0 & 0 & (1/r^{(2)}) \mathbf{B}^{(2)^\top} & \mathbf{R}^{(2)} \end{pmatrix} \tag{B27}$$

and the left inverse of $\mathbf{Q}^{(2)}$ is

$$\mathbf{Q}^{(2)^{-1}} = \begin{pmatrix} \mathbf{I}_{Nd} & 0 & 0 & \\ 0 & \mathbf{B}^{(1)} & 0 & \\ 0 & 0 & \mathbf{B}^{(2)} & \\ 0 & & 0 & \mathbf{R}^{(2)^\top} \end{pmatrix}. \tag{B28}$$

So that, $\mathbf{Q}^{(2)^{-1}} \mathbf{Q}^{(2)} = \mathbf{I}_{N^3 + N^2 + Nd}$. Then, the variational equation can be transformed as,

$$\begin{pmatrix} \dot{\boldsymbol{\xi}} \\ \dot{\boldsymbol{\chi}} \\ \dot{\boldsymbol{\eta}} \end{pmatrix} = \mathbf{Q}^{(2)^{-1}} \begin{bmatrix} \mathbf{S}_2 & -\sigma_1 \mathbf{B}^{(1)} \otimes g^{(1)}(\mathbf{s}, \mathbf{s}) & -\sigma_2 \mathbf{B}^{(2)} \otimes g^{(2)}(\mathbf{s}, \mathbf{s}, \mathbf{s}) \\ -\epsilon \mathbf{C}^{(1)} \otimes Dh^{(1)}(0) & -\epsilon \mathbf{I}_{N^2} & 0 \\ -\epsilon \mathbf{C}^{(2)} \otimes Dh^{(2)}(0) & 0 & -\epsilon \mathbf{I}_{N^3} \end{bmatrix} \mathbf{Q}^{(2)} \begin{pmatrix} \boldsymbol{\xi} \\ \boldsymbol{\chi} \\ \boldsymbol{\eta} \end{pmatrix}, \tag{B29}$$

where again, with a slight abuse, we use the same letter to indicate the new transformed coordinates. Now,

$$\begin{aligned} &\mathbf{Q}^{(2)^{-1}} \begin{bmatrix} \mathbf{S}_2 & -\sigma_1 \mathbf{B}^{(1)} \otimes g^{(1)}(\mathbf{s}, \mathbf{s}) & -\sigma_2 \mathbf{B}^{(2)} \otimes g^{(2)}(\mathbf{s}, \mathbf{s}, \mathbf{s}) \\ -\epsilon \mathbf{C}^{(1)} \otimes Dh^{(1)}(0) & -\epsilon \mathbf{I}_{N^2} & 0 \\ -\epsilon C^{(2)} \otimes Dh^{(2)}(0) & 0 & -\epsilon \mathbf{I}_{N^3} \end{bmatrix} \mathbf{Q}^{(2)} \\ &= \mathbf{Q}^{(2)^{-1}} \begin{bmatrix} \mathbf{S}_2 & -\sigma_1 \mathbf{I}_N \otimes g^{(1)}(\mathbf{s}, \mathbf{s}) & -\sigma_2 \mathbf{I}_N \otimes g^{(2)}(\mathbf{s}, \mathbf{s}, \mathbf{s}) & 0 \\ -\epsilon \mathbf{C}^{(1)} \otimes Dh^{(1)}(0) & -\epsilon / r^{(1)} \mathbf{B}^{(1)^\top} & 0 & 0 \\ -\epsilon \mathbf{C}^{(2)} \otimes Dh^{(2)}(0) & 0 & -\epsilon / 2r^{(2)} \mathbf{B}^{(2)^\top} & \epsilon \mathbf{R}^{(2)} \end{bmatrix} \\ &= \begin{bmatrix} \mathbf{S}_2 & -\sigma_1 \mathbf{I}_N \otimes g^{(1)}(\mathbf{s}, \mathbf{s}) & -\sigma_2 \mathbf{I}_N \otimes g^{(2)}(\mathbf{s}, \mathbf{s}, \mathbf{s}) & 0 \\ -\epsilon \mathbf{L}^{(1)} \otimes Dh^{(1)}(0) & -\epsilon \mathbf{I}_N & 0 & 0 \\ -\epsilon \mathbf{L}^{(2)} \otimes Dh^{(2)}(0) & 0 & -\epsilon \mathbf{I}_N & 0 \\ -\epsilon \mathbf{R}^{(2)^\top} \mathbf{C}^{(2)} \otimes Dh^{(2)}(0) & 0 & 0 & -\epsilon \mathbf{I}_{N^3 + N^2 - 2N} \end{bmatrix} \end{aligned} \tag{B30}$$

From this, we can write $(Nd+2N)$ dimensional coupled master equations and (N^3+N^2-2N) coupled salve equations as

$$\begin{pmatrix}\dot{\boldsymbol{\xi}}\\ \dot{\boldsymbol{\chi}}_M\\ \dot{\boldsymbol{\eta}}_M\end{pmatrix}=\begin{pmatrix}\mathbf{S}_2 & -\sigma_1\mathbf{I}_N\otimes g^{(1)}(\mathbf{s},\mathbf{s}) & -\sigma_2\mathbf{I}_N\otimes g^{(2)}(\mathbf{s},\mathbf{s},\mathbf{s})\\ -\epsilon\mathbf{L}^{(1)}\otimes Dh^{(1)}(0) & -\epsilon\mathbf{I}_N & 0\\ -\epsilon\mathbf{L}^{(2)}\otimes Dh^{(2)}(0) & 0 & -\epsilon\mathbf{I}_N\end{pmatrix}\begin{pmatrix}\boldsymbol{\xi}\\ \boldsymbol{\chi}_M\\ \boldsymbol{\eta}_M\end{pmatrix}. \tag{B31}$$

Here, $(\boldsymbol{\chi}_M,\boldsymbol{\eta}_M)=(\boldsymbol{\chi}_1,\boldsymbol{\eta}_1)$ and the slave equations read as,

$$\begin{pmatrix}\dot{\boldsymbol{\chi}}_S\\ \dot{\boldsymbol{\eta}}_S\end{pmatrix}=\begin{pmatrix}-\epsilon\mathbf{R}^{(2)^\top}\mathbf{C}^{(2)}\otimes Dh^{(2)}(0) & 0 & -\epsilon\mathbf{I}_{N^2-N}0 & -\epsilon\mathbf{I}_{N^3-N}\end{pmatrix}\begin{pmatrix}\boldsymbol{\xi}\\ \boldsymbol{\chi}_M\\ \boldsymbol{\chi}_S\\ \boldsymbol{\eta}_M\\ \boldsymbol{\eta}_S\end{pmatrix}, \tag{B32}$$

where $\boldsymbol{\chi}_S=(\chi_2^\top,\ldots,\chi_N^\top)^\top$ and $\eta_S=(\eta_2^\top,\ldots,\eta_N^\top)^\top$.

Now again, to decouple the coupled master variational equation, we introduce a similar unitary transform like the pairwise adaptation case and introduce the new sets of co-ordinates as,

$$\begin{pmatrix}\mathbf{U}\otimes\mathbf{I}_d & 0 & 0\\ 0 & \mathbf{U} & 0\\ 0 & 0 & \mathbf{U}\end{pmatrix}\begin{pmatrix}\boldsymbol{\xi}\\ \boldsymbol{\chi}_M\\ \boldsymbol{\eta}_M\end{pmatrix}=\begin{pmatrix}\hat{\boldsymbol{\xi}}\\ \hat{\boldsymbol{\chi}}\\ \hat{\boldsymbol{\eta}}\end{pmatrix},$$

with $\mathbf{U}$ the matrix whose columns are the orthonormal eigenvectors that diagonalize the pairwise Laplacian $\mathbf{L}^{(1)}$, i.e., $\mathbf{U}^\top\mathbf{L}^{(1)}\mathbf{U}=\mathbf{D}=\mathrm{diag}\{\mu_1^{(1)},\mu_2^{(1)},\ldots,\mu_N^{(1)}\}$. In terms of the changed coordinate frame the variational equation becomes

$$\begin{pmatrix}\dot{\hat{\boldsymbol{\xi}}}\\ \dot{\hat{\boldsymbol{\chi}}}\\ \dot{\hat{\boldsymbol{\eta}}}\end{pmatrix}=\begin{pmatrix}\tilde{\mathbf{S}}_2 & -\sigma_1\mathbf{I}_N\otimes g^{(1)}(\mathbf{s},\mathbf{s}) & -\sigma_2\mathbf{I}_N\otimes g^{(2)}(\mathbf{s},\mathbf{s},\mathbf{s})\\ -\epsilon\mathbf{D}\otimes Dh^{(1)}(0) & -\epsilon\mathbf{I}_N & 0\\ -\epsilon\tilde{\mathbf{L}}^{(2)}\otimes Dh^{(2)}(0) & 0 & -\epsilon\mathbf{I}_N\end{pmatrix}\begin{pmatrix}\hat{\boldsymbol{\xi}}\\ \hat{\boldsymbol{\chi}}\\ \hat{\boldsymbol{\eta}}\end{pmatrix}, \tag{B33}$$

where $\tilde{\mathbf{L}}^{(2)}=\mathbf{U}^\top\mathbf{L}^{(2)}\mathbf{U}$ and $\tilde{\mathbf{S}}_2=\mathbf{U}^\top\mathbf{S}_2\mathbf{U}$. In explicit form, it can be rewritten as

$$\begin{aligned}\dot{\hat{\xi}}_i=&\left[Df(\mathbf{s})+\sigma_1h^{(1)}(0)r^{(1)}Dg^{(1)}+2\sigma_2r^{(2)}h^{(2)}(0)Dg^{(2)}-\sigma_1h^{(1)}(0)\mu_i^{(1)}D_2g^{(1)}\right]\hat{\xi}_i-\sigma_2h^{(2)}(0)\sum_{j=1}^{N}\tilde{L}_{ij}^2D_sg^{(2)}\hat{\xi}_j\\ &-\sigma_1g^{(1)}(s,s)\hat{\chi}_i-\sigma_2g^{(2)}(s,s,s)\hat{\eta}_i, &\text{(B34a)}\\ \dot{\hat{\chi}}_i=&-\epsilon[\mu_i^{(1)}Dh^{(1)}(0)\hat{\xi}_i+\hat{\chi}_i], &\text{(B34b)}\\ \dot{\hat{\eta}}_i=&-\epsilon[\sum_{j=1}^{N}\tilde{L}_{ij}^2Dh^{(2)}(0)\hat{\xi}_i+\hat{\eta}_i], &\text{(B34c)}\end{aligned}$$

which is the master stability equation we need.